**Naval Research Laboratory**

**Washington, DC 20375-5320**

**NRL/FR/7213--02-9957**

# Opening a New Window on the Universe: High-Resolution, Long-Wavelength Radio Astronomy

NAMIR E. KASSIM
T. JOSEPH W. LAZIO
WILLIAM C. ERICKSON

*Radio/IR/Optical Sensors Branch*
*Remote Sensing Division*

November 25, 2002

## CONTENTS

# EXECUTIVE SUMMARY

Although K. Jansky's (1933) discovery of radio astronomy was at decametric wavelengths, the urgent quest for ever higher angular resolution and the belief that ionospheric structure limited interferometric imaging to short (less than 5 km) baselines caused long-wavelength radio astronomy largely to be abandoned after the initial pioneering work. The long wavelength (LW, taken to be 2 to 20 m or 15 to 150 MHz) portion of the electromagnetic spectrum thus remains one of the most poorly explored regions of the spectrum. Even so, there are a number of important astrophysical questions that can be addressed only by LW observations. In addition, there are problems that may be usefully addressed at a variety of wavelengths, but that may be studied with unparalleled efficiency in the LW regime.

The jointly developed NRL-NRAO 74 MHz observing system has demonstrated (Kassim et al. 1993) that self-calibration techniques can remove ionospheric distortions over arbitrarily long baselines. In its initial year of operation, the system has attracted a wide variety of innovative observing proposals with encouraging initial results in solar system (planetary emission, solar bursts), Galactic (pulsars, supernova remnants), and extragalactic (cluster halos, radio galaxies) astrophysics.

This now presents the exciting opportunity to open efficiently and economically a new high-resolution, high-sensitivity window on the electromagnetic spectrum at the longest wavelengths (Kassim and Erickson 1998). This report describes the scientific justification and initial technical design of the Long Wavelength Array (LWA). The LWA will be a fully electronic, broadband antenna array operating in the 15 to 150 MHz range with a collecting area of 1 $km^2$ at 15 MHz. Because there is no longer an ionospheric limit on baseline length, the longest baselines will be 500 km, providing an angular resolution of $8''$ at 15 MHz and $0.8''$ at 150 MHz. The combination of large collecting area and high resolution will enable the LWA to produce images with sensitivities of order 1 mJy at 15 MHz and 300 $\mu$Jy at 150 MHz. As such, the LWA will represent an improvement of 2 to 3 orders of magnitude in resolution and sensitivity over the state of the art.

A key operational goal of the LWA would be solar observations—both passive imaging and radar imaging. In the latter mode, the LWA would serve as the receiver for bistatic observations of the Sun, with particular emphasis on the imaging of coronal mass ejections (CMEs). At night, the LWA would serve as an astrophysical laboratory to study the origin, spectrum, and distribution of the Galactic cosmic ray electron gas and as a search instrument for high red-shift radio sources—both radio galaxies and star-forming galaxies—and galaxy and cluster halos.

# OPENING A NEW WINDOW ON THE UNIVERSE: HIGH-RESOLUTION, LONG-WAVELENGTH RADIO ASTRONOMY

## 1. INTRODUCTION

### 1.1 Background

Although Jansky's (1933) discovery of radio astronomy was at decametric wavelengths, the urgent quest for ever higher angular resolution and the fact that ionospheric structure limits interferometric imaging to short (less than 5 km) baselines at long wavelengths (LW, taken to be 2 to 20 m or 15 to 150 MHz) has left the LW region among the most poorly explored in the entire spectrum. This is despite the many important astrophysical questions that can be addressed only by LW observations, in addition to those problems that may be usefully studied at a variety of wavelengths, but that may be addressed with unparalleled efficiency in the LW regime. Thus the recent demonstration by the 74 MHz VLA system (Kassim et al. 1993) that self-calibration can accurately remove ionospheric distortions over arbitrarily long baselines now offers the exciting opportunity to efficiently and economically open a new high-resolution, high-sensitivity window on the electromagnetic spectrum at the longest wavelengths (Kassim and Erickson 1998).

The jointly developed Naval Research Laboratory-National Radio Astronomy Observatory 74 MHz observing system came fully on line in 1998 January with all 27 antennas equipped with 74 MHz receivers (prior to this a prototype system was installed on eight antennas). The system has already attracted a wide variety of innovative observing proposals with encouraging initial results in solar system (planetary emission, solar bursts), Galactic (pulsars, supernova remnants), and extragalactic (cluster halos, radio galaxies) astrophysics. Figures 1 to 3 provide dramatic examples of the types of images currently being produced by this system. Figure 1 is an image of the Galactic supernova remnant (SNR) Cas A and provides only the second direct case (after SN 1006, Hamilton and Fesen 1988) of evidence for unshocked ejecta interior to the reverse shock in a young SNR (Kassim et al. 1995b) as predicted by various theoretical analyses (e.g., Lozinskya 1992). Figure 2 is an image of the radio galaxy Virgo A and provides important evidence that the large-scale radio halo is a response to the activity of the black hole-jet system and, contrary to conventional wisdom, is a relatively young feature (Owen et al. 2000). Figure 3 is a deep (rms noise level $\approx 25$ mJy beam$^{-1}$) image of the field containing the Coma cluster of galaxies (Kronberg 1999). The detection of the emission from the steep spectrum halo is important to theories of particle acceleration and magnetic fields in clusters of galaxies. Moreover, the amazing field of view (FoV, greater than $10^\circ$), angular resolution ($\sim 1'$), and sensitivity ($\approx 25$ mJy beam$^{-1}$) provided by this single VLA pointing testify to the dramatic imaging power offered by LW systems.

Now that the ionospheric barrier has been removed, such images can reveal unique information not only for important large-scale emission studies (e.g., SNRs, the Galactic center, galaxy and cluster halos), but also for studies that benefit from high sensitivity to small-diameter steep

Manuscript approved February 28, 2000.

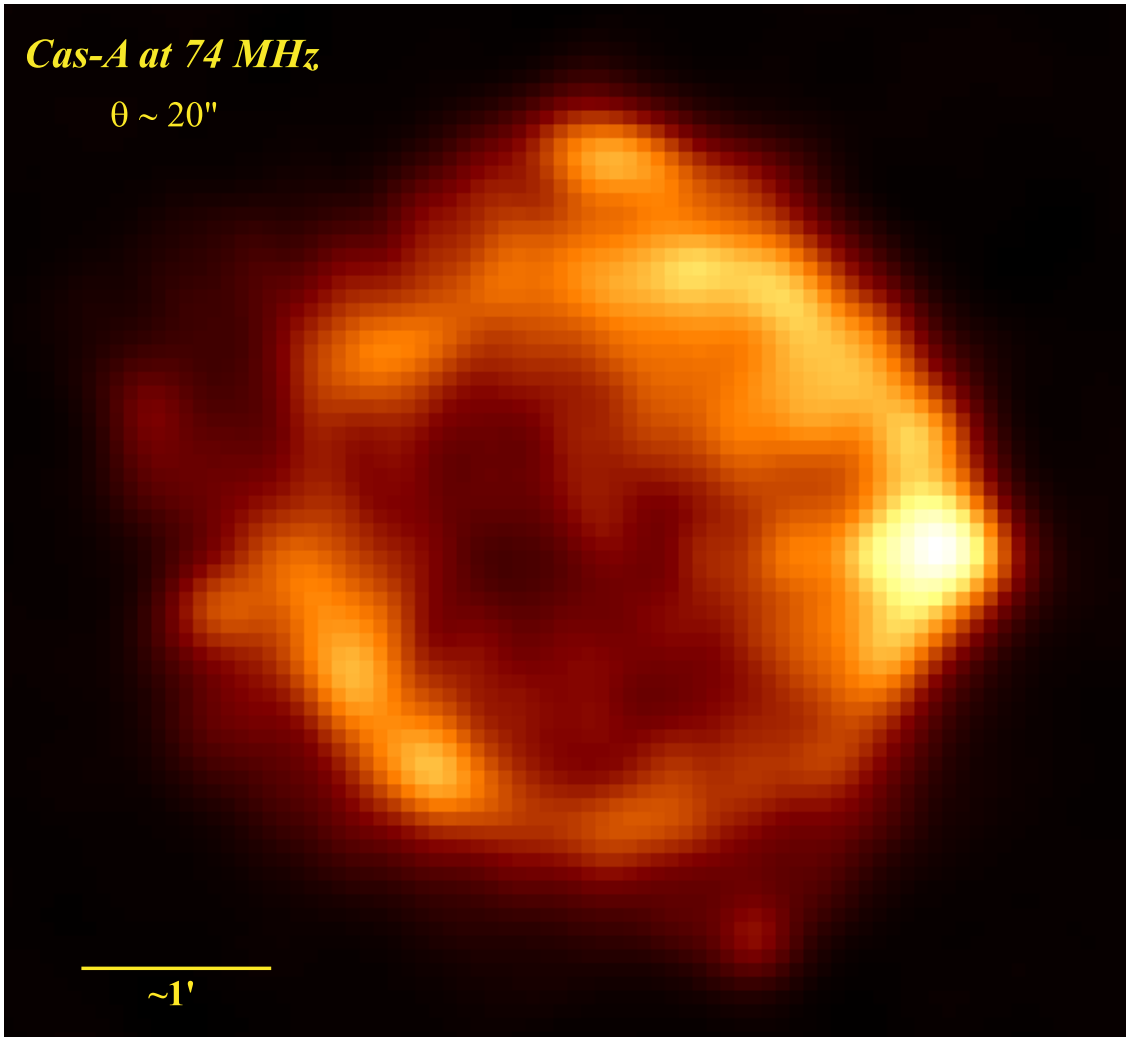


Fig. 1—The supernova remnant Cas A at 74 MHz. This image was made with the prototype, eight-antenna 74 MHz VLA system. This image provided only the second example of unshocked ejecta interior to the reverse shock in a young supernova remnant (Kassim et al. 1995b).

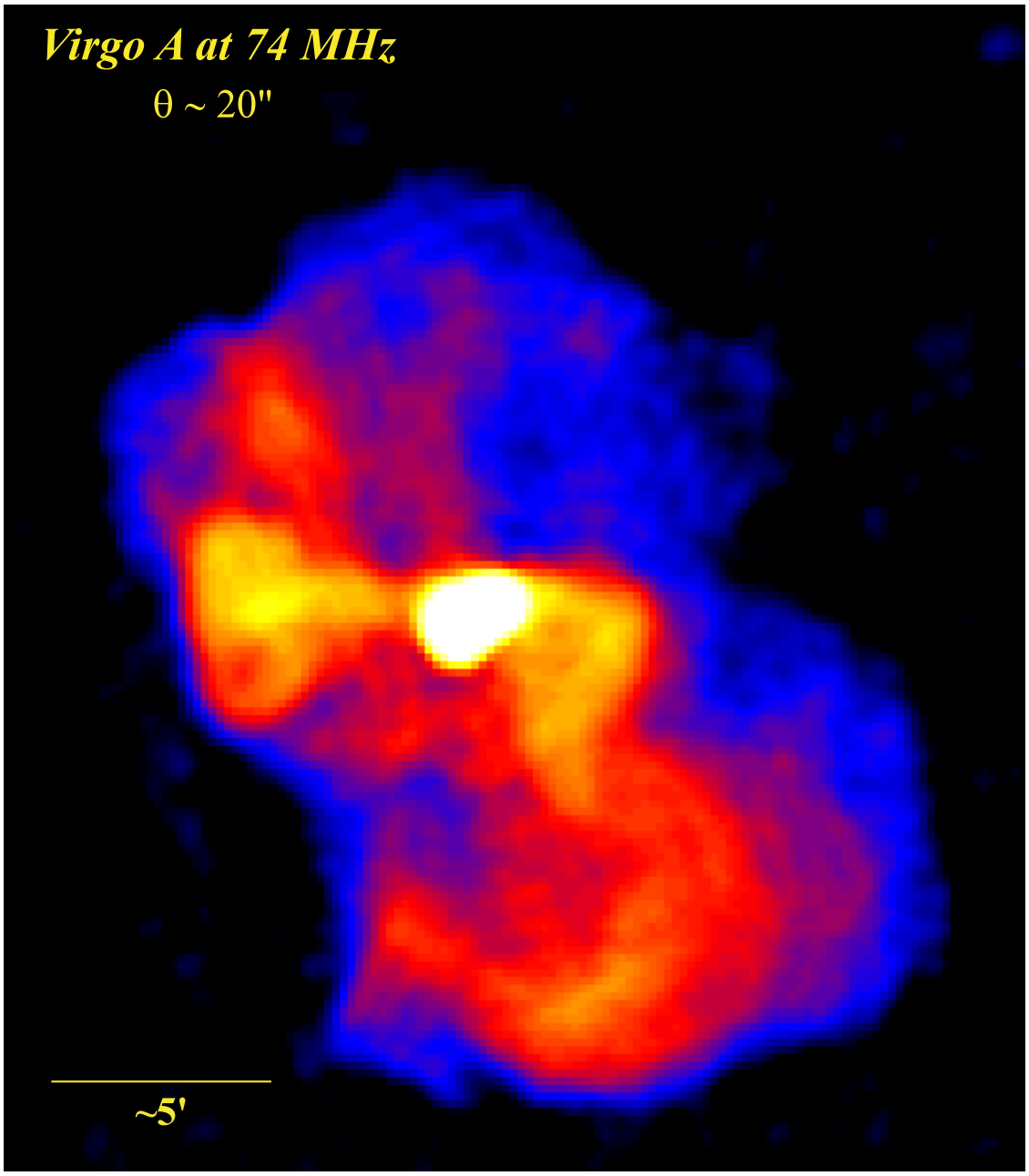


Fig. 2—The active radio galaxy Virgo A at 74 MHz. This figure demonstrates that the large scale radio halo is a response to the activity of the Virgo A black hole-jet system, and, contrary to conventional wisdom, is a relatively young feature (Owen et al. 2000).

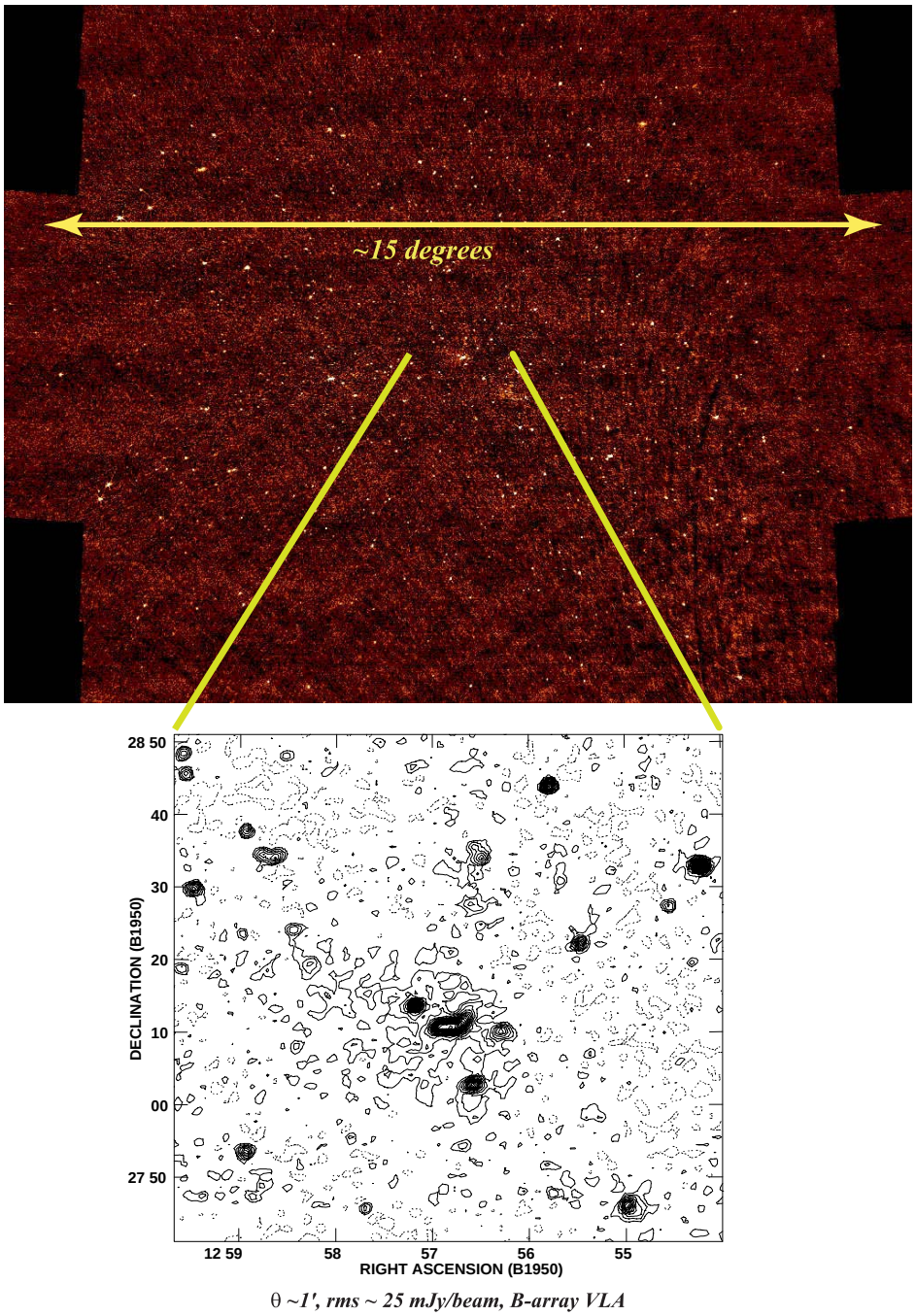


Fig. 3—The Coma cluster of galaxies at 74 MHz. *(Top)* The entire primary beam. This image illustrates the efficiency with which large sections of the sky can be mapped with a sensitive, LW instrument. The rms noise level is 25 mJy beam$^{-1}$, and the FoV covers approximately 15° at a resolution of 1′. *(Bottom)* A subimage of the wide-field image showing the central galaxies and the cluster halo.

spectrum sources (e.g., pulsars and high redshift radio galaxies), which can now be obtained with incredible efficiency. Furthermore, a sensitive, high angular resolution, LW instrument would also be the ideal receiver for solar radar, an innovative concept that could image Earthward-bound CMEs, thereby opening up a new field of space weather research and prediction.

### 1.2 Long Wavelength Array (LWA) Concept

The dramatic successes with the narrow-band VLA system (Kassim et al. 1993) of modest collecting area ($\sim 10^3$ m$^2$) and unprecedented angular resolution ($\approx 20''$) provide strong incentives to develop a much larger ($\sim$ 500 km baselines) and more sensitive ($A_{\rm eff} > 10^5$ m$^2$) instrument. A completely electronic Long Wavelength Array (LWA) could explore the entire LW spectrum at unmatched levels of sensitivity (sub-mJy) and angular resolution (arc-second) (Kassim and Erickson 1998). Moreover, the ability to do this from the ground with intrinsically modest bandwidths and relatively inexpensive hardware permits the array to be developed at a fraction of the cost of higher frequency ground- or space-based systems of comparable size and sophistication. The approximately \$25,000 total cost of the hardware required for the development of the 74 MHz NRL-NRAO system is dramatic testimony to this fact.

Figures 4 and 5 illustrate the landmark improvements the LWA, with its 500-km baselines, could achieve in the LW range over past or present instruments. Figure 4 shows that the LWA will surpass, in most cases by two orders of magnitude or more, the angular resolution of available LW instruments. While a few instruments are edging towards improved angular resolution at a "spot" frequency (e.g., the GMRT at 150 MHz or the VLA at 74 MHz), Fig. 4 shows that the LWA can provide high angular resolution with a broad frequency coverage.

Figure 5 shows that the LWA achieves a parallel breakthrough in sensitivity, even over instruments with comparable collecting areas (e.g., UTR2 with $A_{\rm eff} > 10^5$ m$^2$), reflecting the impact of improved angular resolution on limiting source confusion, a key limit to the sensitivity of LW instruments. The importance of reducing source confusion is demonstrated by the the impressive relative sensitivity of the 74 MHz VLA system, which has a collecting area of only $A_{\rm eff} \sim 10^3$ m$^2$.

Fortunately, collecting area is inexpensive at LWs. This is because simple wire antennas can be mass produced and because system temperatures are dominated by the Galactic background, making low-cost preamplifiers entirely adequate. The modest intrinsic bandwidths also result in very low receiver and associated electronic costs.

Figure 6 shows a possible LWA layout with maximum baselines of order 500 km whose basic building block is a simple, crossed-dipole, log-periodic element. This array design is discussed in more detail in Section 3.

### 1.3 Potential LWA Consortia

Groups at both NRL and the Netherlands Foundation for Research in Astronomy (NFRA), the latter being leaders in Square Kilometer Array (SKA) planning, have a strong interest in developing the LWA. The NRL is interested both for the astrophysics and for potential use of the LWA as a solar radar receiver (Kassim and Erickson 1998). The latter use of the array could open an entirely new area of solar research and, for example, detect Earthward-bound CMEs for accurate

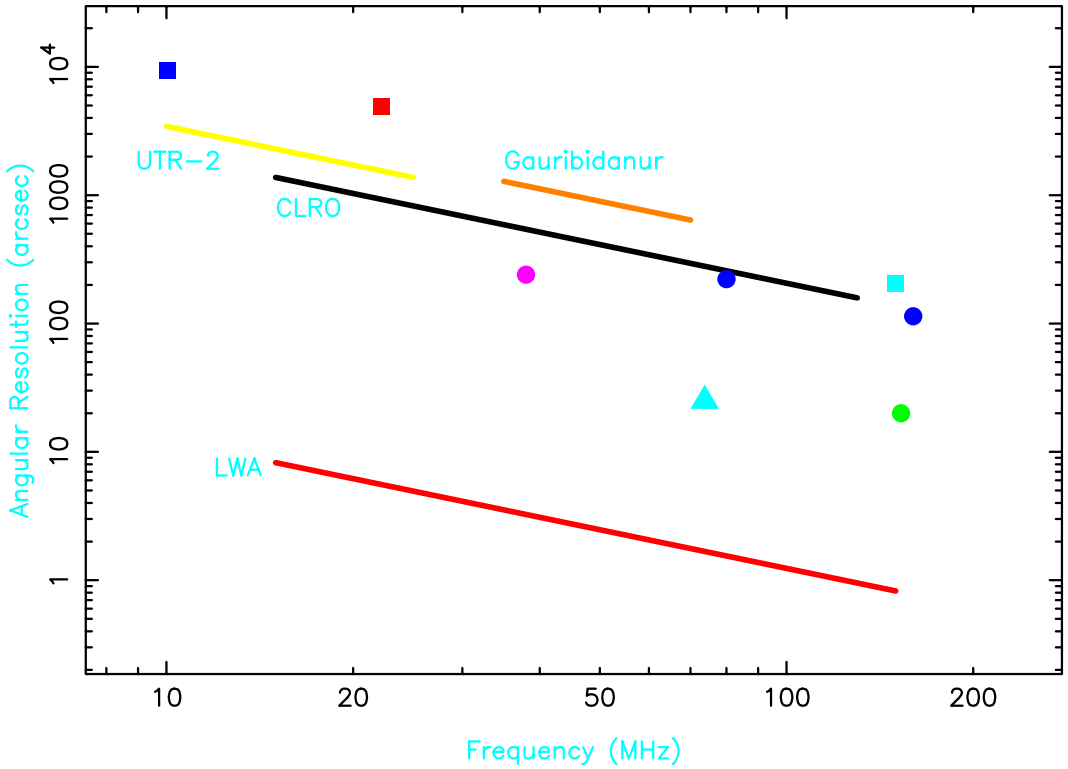


Fig. 4—Angular resolution (arcseconds) as a function of frequency (MHz) for past and present LW imaging instruments in the 10 to 200 MHz range. In addition to the broadband instruments labelled in the figure, various telescopes that operate or operated at "spot" frequencies are shown. These include the Giant Metrewave Radio Telescope (GMRT; green circle), Culgoora (blue circles); the 74 MHz VLA (cyan triangle); Cambridge Polar Cap survey (pink circle); the Dominion Radio Astronomy Observatory at 10 MHz (blue square) and at 22 MHz (red square); and the Mauritius Radio Telescope (cyan square). The LWA will result in a dramatic improvement in angular resolution and frequency coverage.

and economical geomagnetic storm prediction. The solar radar concept has attracted the interest of the National Astronomy and Ionosphere Center (NAIC), as the Arecibo Observatory is an excellent LW solar-radar transmitting candidate. The NFRA is also developing the LWA as the first step towards realizing the SKA.

### 1.4 Structure of this Report

Section 2 presents the scientific justification for developing the LWA, and Section 3 explores the LWA technical concept. The LWA—a broadband, entirely electronic telescope—could be realized at modest cost ($\sim$ \$25 million), indicating that we have an exciting opportunity for a detailed exploration of the wavelength regime where radio astronomy was first discovered. These and our other conclusions are summarized in Section 4.

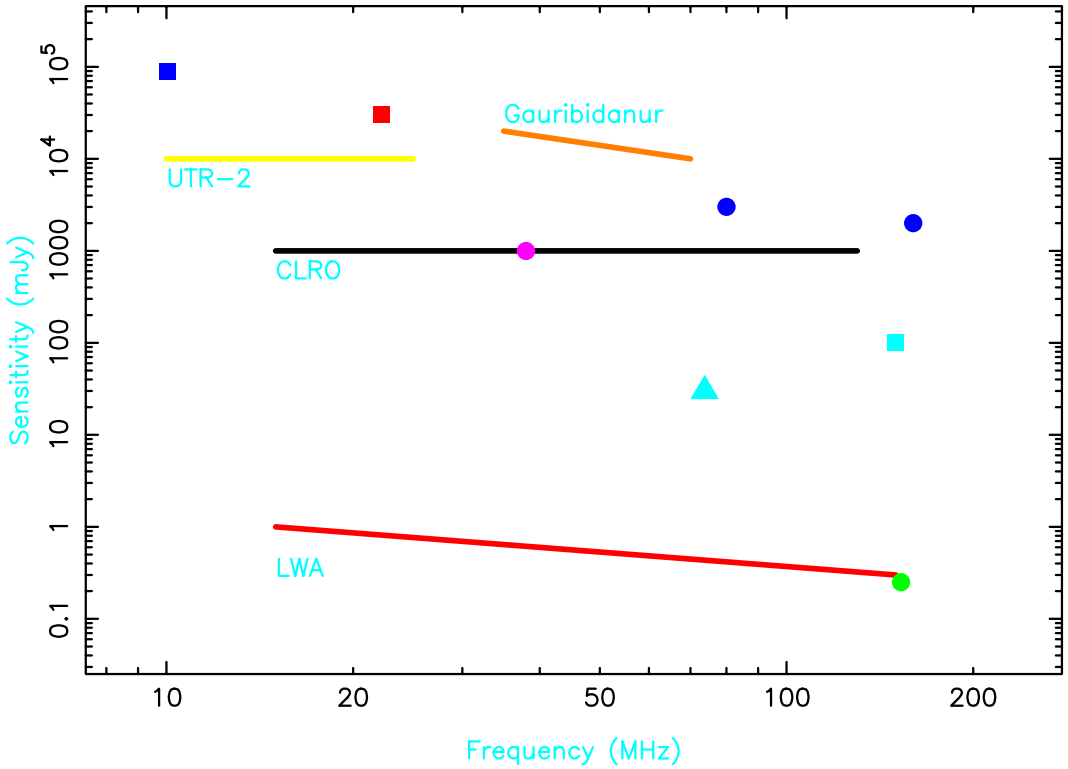


Fig. 5—Sensitivity (mJy) to a point source as a function of frequency for the same instruments shown in Fig. 4. The sensitivities are estimates of the minimum detectable flux density provided by (past, present, and proposed) LW instruments. As in Fig. 4, the LWA will make a dramatic advance in sensitivity at the lowest frequencies. The LWA sensitivity calculation is based on a $\lambda^2$ dependent collecting area assumed to be $10^6$ m$^2$ at 15 MHz. A bandwidth of 3 MHz and integration time of 8 hr have also been assumed.

## 2. LONG-WAVELENGTH SCIENCE

Numerous scientific projects could be carried out by a sensitive, high–angular-resolution, LW instrument. Unrivaled continuum spectra for studies of shock acceleration and spectral aging in Galactic (supernova remnants) and extragalactic (radio galaxies) sources could be produced. High-redshift radio galaxies and quasars, shocks driven by infalling matter in clusters of galaxies, pulsars in the Milky Way and in external galaxies, and radio bursts from nearby stars and extrasolar planets are examples of steep-spectrum processes that could be detected, and in some cases imaged, in large numbers. A frequency versatile system would be capable of distinguishing between intrinsic (synchrotron self-absorption, source variability) and extrinsic (free-free absorption, scattering) physical processes affecting nonthermal emission at LWs. Physical parameters of the ionized interstellar medium (ISM)—cosmic-ray emissivity, emission measure, temperature, pressure, and ionization state—can be constrained from LW observations of H II regions and recombination lines from very high Rydberg state atoms. Below 100 MHz, H II regions become opaque, thereby providing "walls" at known distances allowing distance determinations to various foreground objects, in both the Galaxy and external galaxies. Coherent emissions—from the Sun, the Earth, Jupiter, nearby extrasolar planets, and pulsars—occur primarily at LWs. Finally, an LW system used as a receiver for solar radar transmissions could play an important role in space-weather forecasting.

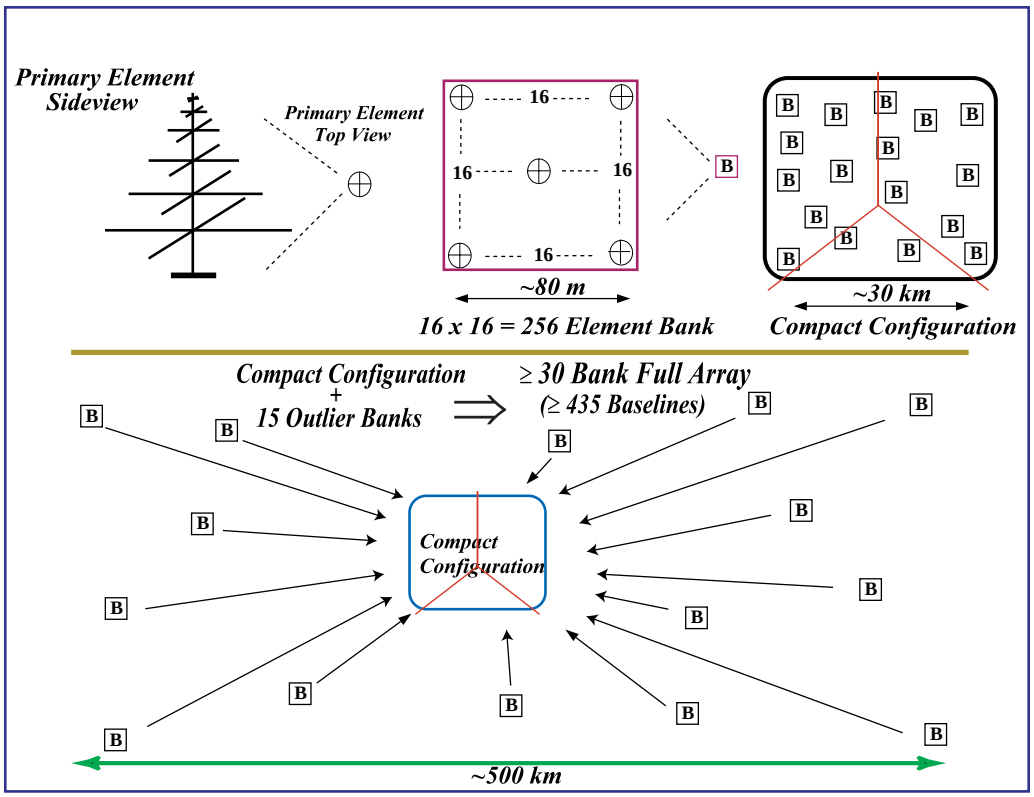


Fig. 6—A strawman Long Wavelength Array layout

### 2.1 Cosmology and Large-Scale Structure

After the Universe recombined at $z \approx 1500$, it was neutral until the epoch of first star formation. Soon after the formation of the first stars, the Universe became reionized, probably on a fairly rapid time scale, around $z \sim 10$ (e.g., Gnedin and Ostriker 1997).

Prior to the epoch of full reionization, the intergalactic medium and gravitationally collapsed systems will be detectable in the 21-cm line of H I (e.g., Tozzi et al. 1999). Physical mechanisms that would produce a 21-cm signature include Ly$\alpha$ coupling of the hydrogen spin temperature to the kinetic temperature of the gas, resulting from radiation by the first generation of stars; preheating by the soft X rays from collapsing dark matter halos; and preheating by ambient Ly$\alpha$ photons. A patchwork of either 21-cm emission and/or absorption against the cosmic microwave background will result. Absorption will occur in the case where the spin temperature of the gas falls below that of the microwave background, as might occur if the spin temperature couples to the gas kinetic temperature through the standard Field mechanism of resonant scattering of Ly$\alpha$ photons. The typical ambient gas kinetic temperature will be lower than the microwave background temperature at high redshift. The expected signals in the redshifted 21 cm line will occur below 200 MHz ($z > 7$).

The signature of the epoch of reionization will be two-fold. On a global scale (i.e., the entire sky), there will be a drop in the sky spectrum near 100 MHz, resulting from the large decrease in

the abundance of neutral hydrogen accompanying reionization. On smaller scales (greater than or equal to $1'$) and in narrower bandwidths (few MHz corresponding to 3000 km $s^{-1}$), there will be emission and/or absorption structures.

Detecting these signatures will be challenging. The expected spectral decrement is about 1% of the amplitude of the cosmic background radiation, and the individual structures will have brightness temperatures of about 50 mK. Nonetheless, it seems possible that the next generation of long wavelength telescopes might be capable of detecting the signature of reionization (Shaver et al. 1999, but see Gnedin and Ostriker 1997).

The LWA would be useful in two respects in a search for the reionization signature. First, the inner portions of the array (Section 3) would be sensitive to emission on sufficiently extended angular scales that the array itself could be used to search for the spectral signature. Second, as Shaver et al. (1999) discuss, a crucial aspect of this experiment will be to identify, model, and remove foreground sources of contaminating signal. One such contaminant is discrete radio sources (i.e., radio galaxies and radio-loud quasars). The long baselines of the LWA would assist in the identification of discrete sources in the FoV being observed for the spectral decrement. In both cases—use of the inner portion of the LWA to search for the spectral decrement and exploiting the high angular resolution of the LWA to identify foreground contaminants—the broadband nature of the LWA will be essential. The epoch of reionization, and therefore the frequency of the spectral decrement, is uncertain. The broadband nature of the proposed LWA would enable a search for this effect over a finely spaced grid of frequencies, increasing the chances of detecting the effect.

If the LWA is able to detect the individual emitting or absorbing structures, it will help constrain the power spectrum of baryonic density fluctuations at $z > 5$, corresponding to the "dark ages," i.e., the transition epoch from the post-recombination Universe to a Universe populated with galaxies. Constraining the power spectrum of gravitationally fragmenting structure at high redshift is fundamental to our understanding of cosmic structure formation, and is one of the few such fundamental parameters that will not be determined by future microwave background anisotropy experiments.

We discuss the identification of fossil galaxies in more detail below (Section 2.2.5). Here, we merely note that the successful identification of fossil galaxies would allow their spatial distribution to be studied. In turn, this spatial distribution may provide constraints on the early epochs of large-scale structure formation. We also discuss the use of radio galaxies as probes of cluster environments in Section 2.2.2.2.

## 2.2 Formation and Evolution of Galaxies

### *2.2.1 Cluster Radio Halos and Intergalactic Magnetic Fields*

A small number of galaxy clusters show radio halos—diffuse, central radio emission not associated with any one galaxy in the cluster. Several models have been proposed to explain the origins of these halos: an injection of relativistic electrons from radio galaxies, in situ particle acceleration due to turbulence, or a merger shock wave and secondary production from hadronic interactions of cosmic ray protons with the intracluster medium (for a review see Schlickeiser et al. 1987). While each model has its advantages, none can explain all of the observed features of radio halos.

In particular, most of the models predict a much higher number of cluster halos than observed. The "missing" halos may have escaped detection by virtue of their steep spectra, suggesting that a search at LWs would find many more halos. Many models also predict that radio halos are a transient phenomena, suggesting that a pool of relic electrons around a few hundred MeV is expected due to a maximum of the cooling time in this energy range (Sarazin 1999). Indirect evidence for the existence of these relic electrons has been found recently as excess extreme ultraviolet emission from clusters (Hwang 1997; Ensslin and Biermann 1998; Sarazin and Lieu 1998; Bowyer and Berghöfer 1998), emission that may be due to inverse Compton scattering of cosmic background photons (Lieu et al. 1996; Bowyer et al. 1996; Bowyer et al. 1998; Mittaz et al. 1998). If the radio synchrotron emission from electrons with energies of order a few hundred MeV can be detected, the combined radio and EUV information would provide a measurement of the magnetic field strength inside the intracluster medium. A comparison of such an estimate with Faraday rotation measurements for the Coma cluster indicates the existence of highly structured magnetic fields (Ensslin et al. 1999).

Long-wavelength measurements of polarized background sources are also a sensitive tool for detecting weak magnetic fields outside clusters of galaxies because of the $\lambda^2$ dependence of Faraday rotation. The high angular resolution and sensitivity of the LWA may enable it, at the higher end of its frequency range, to measure changes in the Faraday rotation across extended, polarized, background sources. The sensitivity of the LWA will increase the number of background sources that can be used to probe the peripheries of any given cluster and will extend studies of the magnetic fields to the peripheral regions of cluster with good statistics for the first time.

Magnetic fields inside clusters of galaxies are expected from phase transitions occurring after the Big Bang, battery effects at shock waves, injection by radio galaxies and galactic winds, and the action of a turbulent dynamo driven by structure formation flows. An understanding of the properties of large-scale magnetic fields is crucial for an understanding of the origin of the observed cosmic ray events above $10^{18}$ eV. These particles are believed to be of extragalactic origin so that they had to travel through the large-scale magnetic fields, which should affect their trajectories (Lemoine et al. 1997, Sigl and Lemoine 1998).

### *2.2.2 Evolutionary Studies of Radio Galaxies*

Radio galaxies are a varied group of objects, ranging from high-luminosity objects extending over megaparsec scales and presumably powered by massive black holes to low-luminosity, relatively small objects powered by star formation. The combination of the high sensitivity and high angular resolution capabilities of the LWA could be brought to bear on a number of outstanding problems in the origin, evolution, and nature of the radio galaxy phenomenon. In this section we survey some of the possible applications of the LWA to the study of radio galaxies.

#### 2.2.2.1 High-Redshift Radio Galaxies

Roughly 10% of powerful active galaxies produce oppositely directed radio jets that transport a vast supply of energy over distances of up to a few megaparsecs. These jets feed synchrotron-emitting lobes for as long as $10^8$ to $10^9$ yr. With luminosities in excess of $10^{28}$ W Hz$^{-1}$ sr$^{-1}$, these objects can be detected at great distances, out to redshifts of 4 to 5 and beyond. The detection of such high-redshift objects is vital to our understanding of the origin of active galaxies since at the

redshifts to which radio galaxies are detected ($z = 4.41$ in the case of 6C*0140+326, Rawlings et al. 1996), for a standard assumed cosmological model, only 1 Gyr has elapsed since the Big Bang. This leaves little time for jet-producing central engines and host galaxies to form.

The high-redshift ($z > 3$) radio galaxies known to date are characterized by very steep spectra ($\alpha < -1$) and small angular sizes (less than or roughly equal to $30''$). These characteristics have been exploited in "filtered" samples of radio galaxies; for example the 6C* sample (Blundell et al. 1998) cross-matched sources from the 151 MHz catalogue of Hales et al. (1993) with a 5 GHz survey to obtain a set of sources with very steep spectra. This procedure led to the detection 6C*0140+326, the currently most distant known radio galaxy ($z = 4.41$, Rawlings et al. 1996). The steep spectrum emission of these high-redshift radio galaxies ultimately limits the utility of a survey at 151 MHz; such a survey selects objects at a redshift $z$ according to their surface brightness at a rest-frame frequency of $(1 + z)\,151$ MHz. For example, in the case of an object at a redshift of 6, the survey would select rest-frame emission near 1 GHz. Above 1 GHz, radio galaxy lobes are subject to synchrotron losses, and in addition their lobes suffer inverse Compton losses off the cosmic background radiation, whose energy density increases as $(1 + z)^4$. In order to produce a more complete sample of the high-redshift universe of active galaxies, it is essential to lower the finding-frequency—a task to which the LWA is ideally suited.

The class of low-luminosity radio galaxies with limb-darkened outer structures (Fanaroff-Riley I objects; Fanaroff and Riley 1974), like Virgo A, have typical 1.4 GHz luminosities of $10^{23}$ to $10^{25}$ W Hz$^{-1}$. With spectral indices as steep as $-0.8$, one should be able to detect FR I radio galaxies at 5 mJy flux levels at 74 MHz out to $z = 3$. Moreover, high-$z$ FR I galaxies tend to be diffuse, suggesting that they have much lower magnetic fields than $z = 0$ galaxies. Detection of these sources is particularly interesting because inverse Compton losses scale as $(1+z)^4$ so that, combined with the weaker magnetic fields, inverse Compton losses should become increasingly important at high $z$ with attendant changes in the properties of these galaxies. Thus, for FR I galaxies, steep spectra and radio morphology might be a much stronger filter for high-$z$ objects than for FR II galaxies. Current telescopes can begin to explore the possibility of detecting high-$z$ FR I radio galaxies, but higher resolution and sensitivity are required to study the effect of inverse Compton losses on these objects.

De Breuck et al. (1998) have also recently discovered a new class of ultra–steep-spectrum, very reddened, dusty quasars. Long-wavelength observations would be an efficient means of finding additional objects of this nature.

#### 2.2.2.2 Radio Galaxies as Cluster Probes

In addition to being interesting in their own right, high-$z$ radio galaxies can also serve as probes of cluster "weather," that is the dynamical state of clusters. If one can image some of these objects at high $z$, then one can get an indication of the dynamical state of clusters at earlier epochs and thus their evolution.

For instance, the recent analysis of LW images of Virgo A (Owen et al. 2000) indicates that the black holes in cluster cores may compete with the "cooling flow" from the large-scale cluster atmosphere to control the physics in the inner 100 kpc of rich clusters. One might also expect such sources to be longer lived at lower frequencies, and thus show more about the history of

such processes through their frequency of occurence, structure, and spectral properties at lower frequencies. Since such sources often have very steep spectra ($-2.0$ at meter wavelengths), one might hope to detect such sources to very high redshifts and also be able to make a complete census of well-studied clusters nearby.

#### 2.2.2.3 Emission Mechanisms and Jet Physics

Estimates of the energy budget for radio galaxies are currently hindered by ignorance about the nature and location of the low-energy cutoff of the particle reservoir of the synchrotron-emitting lobes, to the extent that there is over an order of magnitude uncertainty in the values of the jet powers inferred in this way. The secure detection of a *long-wavelength* cutoff or turnover would strongly constrain these calculations. The location of the low-energy cutoff is the cornerstone of the recent result of Wardle et al. (1998) that jets must contain a significant population of light pairs ($e^{\pm}$), rather than heavy pairs ($p^{+}$ and $e^{-}$). This is a key question in astrophysics today, since the composition of the jet material pertains to the nature of the black hole jet-producing mechanism.

Using steep-spectrum radio galaxies and quasars as beacons of the distant universe has many advantages (e.g., radio emission does not suffer obscuration by dust), but basing secure cosmological conclusions on them can only be done if the astrophysical mechanisms by which these objects are governed is understood. Studies of Cygnus A have demonstrated the importance of the LW observations (at 1 and 2 m) in anchoring such studies (Carilli et al. 1991). Previous observations (Myers and Spangler 1985; Alexander and Leahy 1987) have shown a strong spectral-index gradient that steepens from the hotspots back to the core, which may be interpreted as increasing synchrotron losses impacting on the the oldest emitting particles. Such observations confirm the basic models that describe the transport of relativistic particles along collimated jets from the active cores to the hotspots which subsequently feed the radio lobes (Blandford and Rees 1974; Scheuer 1974). However, even a quarter of a century later, the role played by the hotspots in governing the energy supply to the lobes (Blundell et al. 1999) and the lobe-aging processes (Rudnick et al. 1994) have barely begun to be understood. Understanding these are vital, however, for explaining such trends as the strong dependency of spectral index on source luminosity (Heeschen 1960; Laing and Peacock 1980; Blundell et al. 1999). The LWA could observe in the frequency regimes rarely afflicted by synchrotron cooling. The observations would be useful in discriminating between the initial energy distribution supplied by the hotspot and subsequent loss mechanisms as the lobe evolves.

For FR I objects like Virgo A, the very sense of the spectral index gradient is reversed relative to high-luminosity radio galaxies with edge-brightened outer structures (FR II sources), since the energy of the jets is dissipated along their lengths (FR I) instead of at their ends (FR II). Both 74 and 330 MHz observations of Cygnus A (FR II type) and Virgo A have demonstrated these principles (Carilli et al. 1991; Kassim et al. 1993, 1995a). Furthermore, the sharp boundary of the radio halo around Virgo A at 74 MHz (Fig. 2) is evidence that this large scale structure is a response to the activity of the black hole-jet system and is a relatively young feature (Owen et al. 2000). The sensitivity and resolution of the LWA would expand such studies beyond the nearest, brightest, and perhaps atypical, sources.

#### 2.2.2.4 Star Forming Galaxies

Below $10^{23}$ W Hz$^{-1}$ at 20 cm, the radio sky is dominated by starforming galaxies. At luminosities of $10^{23}$ W Hz$^{-1}$, a spiral galaxy has a star formation rate of about 50 M$_\odot$ yr$^{-1}$. At luminosities of $2 \times 10^{21}$ W Hz$^{-1}$, the star formation rate is 1 M$_\odot$ yr$^{-1}$, comparable to that in the Galaxy. For centimeter wavelengths, particle lifetimes are similar to the stellar evolution timescales; this similarity probably accounts for the very good correlation between radio and far infrared emission. However, one might expect that at longer wavelengths, the particle lifetimes would be longer, and "relics" of previous star formation episodes would be visible. Thus, more galaxies should show star-formation–related emission at longer wavelengths. If this is not the case, then there must be an as-yet unknown process responsible for eliminating the particles from the galaxies.

Little is known about the spectral properties of these systems at high redshifts. The same arguments that apply to FR I and II radio galaxies apply to these systems. Hence, for typical galactic magnetic fields, one would expect significant spectral steepening and generally steeper spectra for distant star forming galaxies than nearby ones. The sensitivity of the LWA would enable study of these objects at $z \simeq 0.03$, for a Milky Way-like object, with a normal spectral index. Of course, there may be absorption in the neighborhood of these star forming galaxies. The broadband nature of the LWA would be essential in discriminating between emission from the star-forming process and absorption.

### *2.2.3 Galaxy Halo Emission*

Synchrotron radio halos have been predicted around all types of individual galaxies and clusters of galaxies but have been detected reliably only in rare instances (Kronberg 1990). In normal spirals, the radiation should result from cosmic ray electrons that diffuse or convect out of the disk, and its interpretation bears on questions of cosmic ray origin and transport. In starbursts and Seyferts, high-energy electrons may be funneled away from the nucleus by a disk or be physically transported by jets. In all cases, LW observations are critical because they are excellent tracers of large-scale structure and because the physics underlying the radiation losses suffered by the transported electrons is revealed through the sense of the spectral-index gradients, as is the case of the radio galaxies. Such measurements could be crucial to the interpretation of X-ray halos since, for example, if the X-ray halo recently detected around the edge-on spiral NGC3628 is produced by synchrotron emission, then a steep-spectrum radio halo should also be present.

It is usually difficult to distinguish halo emission from disk emission, and the emission from the galactic disks probably confused most early reports of halo emission. Observations of edge-on galaxies are of particular relevance since, in these cases, disk and halo radiation can be clearly distinguished. The halo emission that has been found in some edge-on galaxies has been attributed to cosmic-ray particles that have been convected out of the disk by gas ejected in superbubbles generated by vigorous starburst activity (Werner 1988). This topic is of great importance in cosmic-ray physics since it pertains to the storage and propagation of cosmic rays in the environment of galaxies, and it also contributes to our understanding of disk-halo interactions in galaxies. The radio spectra of the halos are often steeper than those of the disks, as would be expected for old electrons spiraling in weak magnetic fields. Although LWs are the most appropriate for the study of halo emission, sufficient angular resolution and sensitivity have not been available to conduct such work. A major advantage of LW observations is that they are potentially powerful discriminators

of convective and diffusive halo models. Most models of convection-dominated halos predict a low-frequency flattening that should be easily visible (Lerche and Schlickeiser 1982a, 1982b).

### *2.2.4 Emission and Absorption Mechanisms in Galaxies*

A variety of absorption processes is expected to occur in and around radio galaxies at LWs. These include synchrotron self-absorption, Razin-Tsytovich suppression, turnovers caused by low-energy cutoffs in electron energies, and absorption by thermal gas. All of these mechanisms exhibit different spectral signatures, emphasizing the importance of the broadband LWA. While evidence for the existence of these processes, based on turnovers in integrated low-frequency spectra, has existed for some time, poor angular resolution has prevented essentially all but the simplest conclusions. For instance, 151 MHz observations support the conclusion that the flattening of the hot spot spectra in Cygnus A is due to a low-energy cutoff in the radiating electrons and not to thermal or synchrotron absorption (Carilli et al. 1991). However, the poor angular resolution of the present 74 MHz VLA prevents a definitive test of this conclusion (Kassim et al. 1995a). The LWA would measure the entire low-frequency hotspot spectrum that is vital for understanding how the hotspot governs the energy distribution to the lobe.

In normal galaxies, such as M82, Wills et al. (1997) detected an unexpected free-free absorption of SNRs by giant H II regions at relatively higher frequencies (151 and 408 MHz) than those seen toward Galactic SNRs (Kassim 1989). Such measurements place constraints on the radial location of the discrete nonthermal sources relative to the ionized component of the host galaxy ISM. VLA and Westerbork observations at 330 MHz and MERLIN observations at 151 and 408 MHz can search for such effects, but longer wavelength observations are more sensitive to absorption. The arc-second resolution of the LWA is needed for such studies. On larger scales, the integrated spectra of many normal spiral galaxies appear to flatten near 100 MHz. This flattening may be due to free-free absorption by cool ISM gas (Israel and Mahoney 1990; Hummel 1991; Israel et al. 1992) and could be explored far better with the LWA.

### *2.2.5 Fossil Galaxies*

Synchrotron aging of a relativistic electron population preferentially depletes the high-energy electrons first. Low-energy electrons, which radiate at LWs, have the longest lifetimes. This has prompted speculation about populations of electrons whose radiation lifetimes exceed the Hubble age and has led to the suggestion of the existence of extremely steep-spectrum "fossil galaxies." Estimates of the energy release during the first epochs of radio galaxy activity suggest that these fossil galaxies should be relatively common in the intergalactic medium (Ensslin et al. 1998b). If such fossil galaxies do exist, the proposed LWA would be ideal for detecting them. In addition to information about the oldest electron populations, such observations could provide valuable information about intergalactic or primordial magnetic fields.

Ensslin et al. (1998a) have recently suggested that so-called "cluster radio relics" in the vicinity of clusters of galaxies are in fact such fossil galaxies with a shock-accelerated relativistic electron population. The necessary shock waves would be megaparsecs in scale and could be due either to steady accretion of matter onto the cluster of galaxies or due to a merger event with another cluster (e.g., Abell 2256). Recently observed substructures in X-ray temperature maps support the existence of extended strong shock waves at the locations of several of the known cluster radio relics

(Abell 85, Markevitch et al. 1998; Abell 1367, Donelly et al. 1998; Abell 2256, Roettiger et al. 1995; Abell 3367, Markevitch et al. 1999). Figure 7 shows an example of these proposed shocks around the X-ray cluster Abell 3667; both (thermal) X-ray emission from the cluster core and 843 MHz radio emission from the shock-accelerated electron population in the presumed infalling matter shocks are visible.

Reactivated fossil galaxies are a powerful tool to investigate properties of the infalling matter onto clusters of galaxies and are a test ground for large-scale structure formation. They are steep-spectrum sources, especially if the shock is weak, so that LW observations are required in order to detect more of them. An observation of a reactivated fossil galaxy at the weaker accretion shock at the boundary of a sheet or filament of galaxies would be very challenging for cosmology and only expected to be successful at very LWs.

## 2.3 Interstellar Processes

### *2.3.1 The Origin of Cosmic Rays*

#### 2.3.1.1 Overview

The holy grail of cosmic-ray physics is the answer to the question of their origin. This problem remains unsolved some 87 years after the discovery of cosmic rays by Hess (1912). Viable cosmic-ray origin theories did not even appear for some 65 years. Since then, our understanding of cosmic-ray properties has grown enormously. We now know that cosmic rays are mainly atomic nuclei and electrons that have been accelerated to energies greater than their rest mass energies. They follow a nonthermal power-law distribution with a differential energy index of approximately 2.5. Their energy density in space is of order 1 eV cm$^{-3}$, which translates into a number density of $10^{-9}$ cm$^{-3}$. Thus, cosmic rays can be collectively characterized as a *collisionless, nonthermal gas.*

Table 1 compares the properties of this nonthermal gas with that of other components of the ISM. Column 1 lists the various phases of the ISM. Approximate filling factors are shown in column 2. The number density is shown in column 3. The kinetic energy per particle from each phase is shown in column 4 in electron volts. Column 5 lists the energy density of each phase.

Table 1—Components of the ISM

| Phase | $f$ | $n$ (cm$^{-3}$) | $kT$ (eV) | $nkT$ (eV cm$^{-3}$) |
|---|---|---|---|---|
| Molecular Clouds | $10^{-3}$ | $> 100$ | $< 10^{-2}$ | - |
| Cold Neutral Medium | 0.025 | 40 | $\approx 10^{-2}$ | $\approx 0.4$ |
| Warm Neutral Medium | $\approx 0.5$ | $\approx 0.5$ | $\approx 1$ | $\approx 0.5$ |
| Warm Ionized Medium | $\approx 0.25$ | $\approx 0.2$ | $\approx 1$ | $\approx 0.2$ |
| Hot Ionized Medium | $\approx 0.2$ | $\approx 3 \times 10^{-3}$ | $\approx 10^{2}$ | $\approx 0.3$ |
| Cosmic Rays | $\approx 1$ | $\approx 10^{-9}$ | $\approx 10^{9}$ | $\approx 1$ |

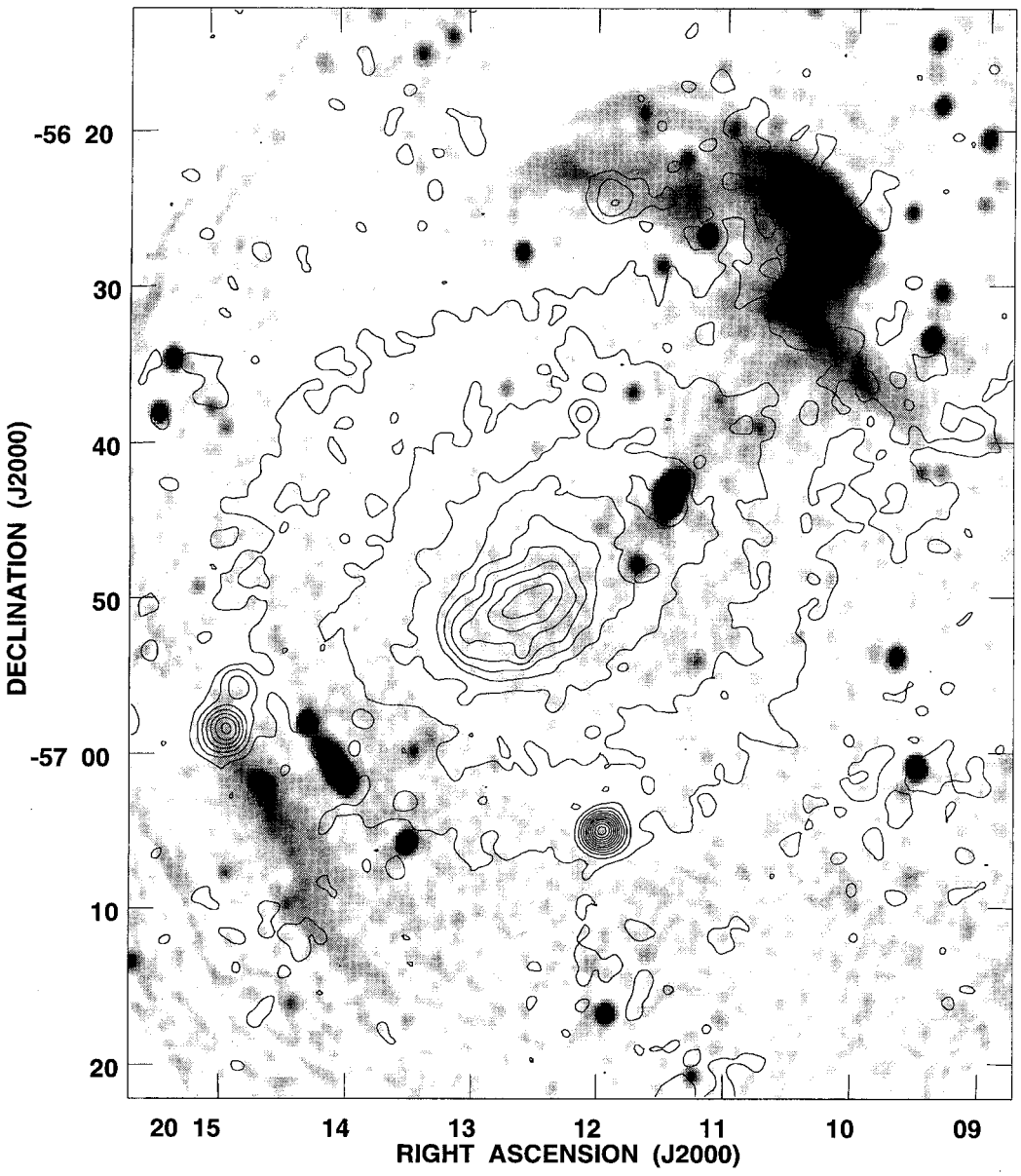


Fig. 7—Steep spectrum halo emission from Abell cluster 3667. A contour representation of the ROSAT PSPC image (0.1 to 2.4 keV) of Abell 3667, overlaid on a grayscale of a wide-field 843 MHz MOST image (Röttgering et al. 1997). The steep-spectrum radio emission may be the shocks formed between infalling matter and the cluster core.

Cosmic rays are energetically important, *containing at least as much energy as the other phases of the ISM*. They therefore play an important role in the evolution of the ISM and should be considered as a legitimate phase of the ISM worthy of detailed study.

#### 2.3.1.2 Measuring Galactic Cosmic Rays

Being charged particles, cosmic rays are easily deflected by Galactic, interplanetary, and geophysical magnetic fields. It is therefore generally impossible to deduce the origin and complete spectrum of the cosmic-ray particles from direct measurements. There is, however, a wide array of measurement tools available for studying Galactic cosmic rays indirectly. Table 2 summarizes the most commonly used tracers of the global distribution of cosmic rays. Column 1 lists the cosmic-ray component that is probed. The mechanism by which the component is detected is shown in column 2. Column 3 shows the component of the ISM with which the mechanism is associated. The range of energies of the cosmic ray particles contributing to the observed emission is shown in column 4. The quantity actually represented by the observed emission is shown in the last column.

Table 2—Global Measurements of Cosmic Rays

| Components | Tracer | Related ISM Component | CR Energy Range | Quantity Measured |
|---|---|---|---|---|
| Electrons | Radio Synchrotron | Magnetic Field | 0.2–10 GeV | $\int n_{\rm CR} B^{1.8}\, dr$ |
| Electrons | Radio Bremsstrahlung | Thermal ISM | 0.1–0.3 GeV | $\int n_{\rm H} n_{\rm CR}\, dr$ |
| Electrons | $\gamma$-ray Inverse Compton | Photons | $< 0.1$ GeV | $\int n_{*} n_{\rm CR}\, dr$ |
| Protons | $\gamma$-ray $\pi^0$ Decay | Thermal ISM | 0.3–10 GeV | $\int n_{\rm H} n_{\rm CR}\, dr$ |

It is clear that multiple tools exist for tracing cosmic rays in the Galaxy. However, it is also obvious that all global tracers of cosmic rays are tied to other components of the ISM and that no global tracer measures the cosmic rays directly. Furthermore, examination of Table 2 shows that there is little overlap in electron energies among the three electron tracers. In fact, there is *no* overlap between cm-wave radio emission and the two $\gamma$-ray tracers. This absence of overlap is illustrated in Fig. 8 (from Longair 1990).

However, at the lower radio frequencies ($\approx$ 10 to 30 MHz), relativistic electrons with $E \approx 200$ to 300 MeV are traced under typical interstellar conditions. This is a region of the energy spectrum that is impossible to study through direct detections because of solar modulation. These same electrons also radiate relativistic bremsstrahlung at the lower $\gamma$-ray photon energies (Table 2). Consequently the quantities in column 5, rows 1 and 2 of Table 2 can be combined (in conjunction with the well-established database of Galactic H I emission) to determine uniquely the distribution of cosmic-ray electrons in the Galaxy, *separately from the magnetic field distribution*, a key problem in understanding the origin of cosmic rays.

Though LW radio astronomy paved the way for opening up the field of cosmic-ray astrophysics, it has had a relatively minor role to play since the pioneering efforts of Jansky (1933) and Reber (1940). The major reason for the irrelevancy of LW radio astronomy to cosmic-ray studies

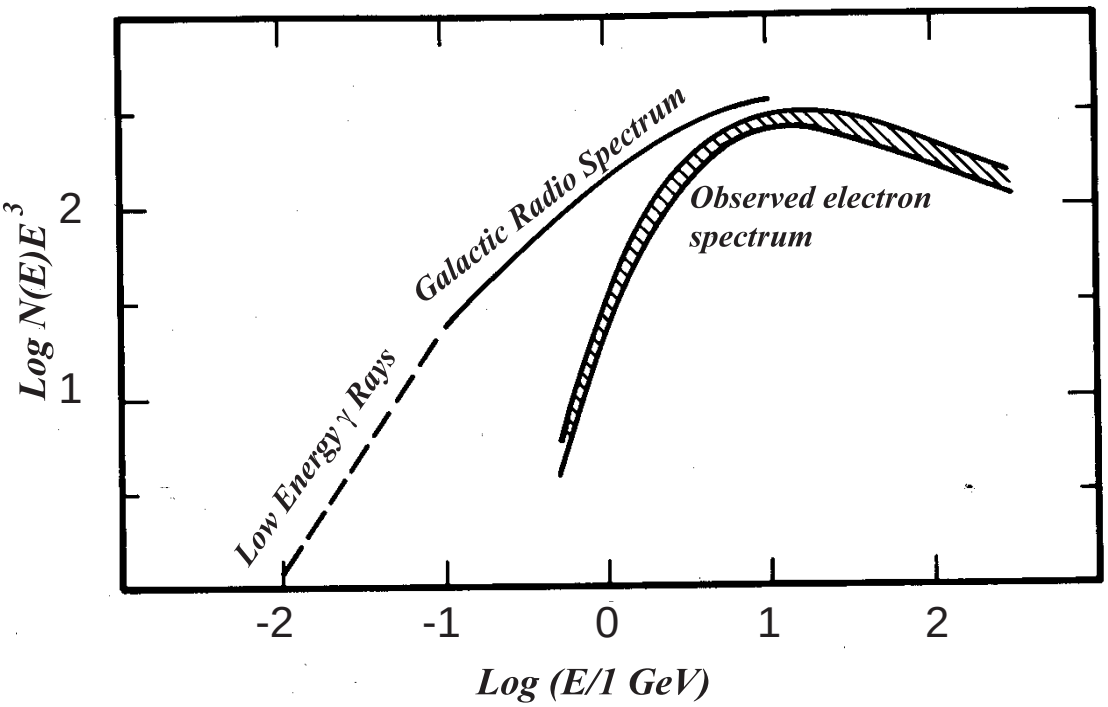


Fig. 8—The spectrum of relativistic electrons in the local ISM (Longair 1990). The directly observed electron energy spectrum is shown in the hatched area. Modulation by the solar wind prevents direct measurement of the intrinsic spectrum below roughly 10 GeV. The electron spectrum derived from the spectra of the Galactic LW radio emission (solid line) and low energy gamma ray emission (dashed line) are also shown. There is no overlap between the radio observations and the $\gamma$-ray observations.

has been the limitations imposed by the Earth's ionosphere. However, with advances being made in phase-calibration and phase-transfer techniques (e.g., Kassim et al. 1993), there are no longer any technological obstacles to building an array capable of tackling the cosmic-ray problem.

The key questions that relate to a full understanding of Galactic cosmic rays are the following:

- How are cosmic rays distributed in space?
- How are cosmic rays accelerated?
- What are the energetics of Galactic cosmic rays?

LW radio astronomy has the potential to provide answers to each of the above questions, as detailed below.

#### 2.3.1.3 Distribution of Cosmic Rays in the Galaxy

All sky surveys at (cm-wavelength) radio and $\gamma$-ray wavelengths show similar emission morphologies. Haslam et al. (1981) compared the (latitude-averaged) longitudinal distribution of (COS-B) $\gamma$-ray and radio emission. Although the profiles differ substantially in directions of specific

sources such as Cas A, Vela, and the Galactic center, the overall distributions, reflecting the diffuse emission, are remarkably similar, even showing enhancements along the spiral arm tangents. The $\gamma$-ray data measure the integral product of cosmic rays and thermal gas along a given line of sight (Table 2, column 5) while the radio data represent the same for cosmic-ray electrons and magnetic fields. Thus, the above similarities could represent the cosmic ray distribution but they could equally well represent a correlation of gas and magnetic fields. A further complicating factor is that cm-wavelength radio emission traces GeV electrons while the $\gamma$-ray (relativistic bremsstrahlung) emission traces sub-GeV electrons.

As discussed earlier, LW radio emission from the ISM traces the same sub-GeV electrons (for frequencies less than 100 MHz). Consequently, a comparison of LW radio emission with mid-energy $\gamma$-ray emission, in conjunction with H I emission, should yield a much improved estimate of the cosmic-ray distribution. A favorable consequence of estimating the cosmic-ray distribution is that the line-of-sight–averaged magnetic field can then be estimated by inverting the synchrotron quantity (Table 2, row 1).

At radio frequencies of 10 to 100 MHz, H II regions become optically thick. Observations of LW synchrotron emission in the direction of such remnants offers a unique opportunity to measure synchrotron emissivity along columns whose lengths are given by the distances to the H II regions. It may therefore be possible to build a three-dimensional model of the electron distribution in the Galaxy. Such a model would offer new insights into the geometry of the Galactic cosmic-ray disk and/or possible halo.

#### 2.3.1.4 The Acceleration of Cosmic Rays

The current paradigm holds that high-energy phenomena, related to supernovae and/or active galactic nuclei (AGNs), are the sources of cosmic rays. However, no direct connection between the particles that we observe locally and any identified cosmic sources has been made, leaving their origin uncertain.

As early as the 1930s, Zwicky (1939) suggested that supernovae were somehow responsible for the acceleration of cosmic rays. This idea was proposed even before the connection between cosmic rays and galactic radio emission was made. Although the supernova idea was much closer to the currently accepted view of cosmic-ray acceleration, it was recognized quite early that strong adiabatic losses prevented significant particle acceleration during the supernova expansion. Instead, it was proposed that it is the interaction of the supernova remnants with the ISM that leads to the acceleration of cosmic rays. The idea was first developed by Bell (1978a, b) using the concept of first-order Fermi acceleration. Subsequent work has evolved this idea into what is currently known as diffusive shock acceleration (DSA). DSA is fully reviewed by Ellison et al. (1994) and, to a lesser extent but more recently, by Jones et al. (1998).

The DSA mechanism in conjunction with SNRs appears to be able to account for the vast majority of cosmic rays (those with energies $\approx 10^9$ to $10^{15}$ eV). However, the classic problem of the injection mechanism (the ability to accelerate seed particles from the thermal pool) remains unsolved (see, Ellison et al. 1994; Jones et al. 1998). A separate mechanism is required to energize particles to sub-GeV energies in order to inject the necessary seed particles into the DSA environment. Long-wavelength radio astronomy is ideally suited for addressing this problem. In supernova

remnants (SNRs), where magnetic fields range from 10 $\mu$G to 1 mG, the synchrotron-emitting electrons have significantly lower energies at a given critical frequency. At 10 to 30 MHz, the electrons span the energy range of 15 to 750 MeV, exactly the range needed to study the nature of the injection mechanism. The shape of the electron spectrum and the spatial correlation of hot-spots with shock features, at these energies, would provide robust constraints on the mechanism that accelerates seed particles in SNRs.

#### 2.3.1.5 Energetics of Cosmic Rays

An important constraint on cosmic-ray origin is the energy density of cosmic rays in the Galaxy. Knowing the distribution of cosmic-ray energy densities in the ISM makes it possible to estimate the energy budget of Galactic cosmic rays. Any plausible sources of cosmic rays must be consistent with such an energy budget.

Direct measurements of cosmic ray fluxes at the top of the Earth's atmosphere suggest that the energy density of cosmic rays is about 0.5 eV cm$^{-3}$. However, this number is a lower limit because the flux is reduced by the outflowing solar wind that strongly modulates the cosmic-ray flux, particularly below about 1 GeV. *Pioneer* and *Voyager* spacecraft have been making in situ measurements of cosmic-ray fluxes as they proceed out of the solar system (e.g., Webber 1990). Their measurements indicate that the energy density of cosmic rays is slowly increasing with distance from the Sun. At 70 AU, the value is about 1.5 eV cm$^{-3}$. The spacecraft have not yet reached the heliospheric boundary. When they do, they will be making measurements in the true ISM, local to the Sun.

Unfortunately, these direct measurements are very local and do not tell us about the energy densities of cosmic rays in other regions of the Galaxy. The energy densities have to be inferred from the synchrotron emission of the relativistic electrons. Interpretation of the synchrotron all-sky maps by Beuermann et al. (1985) suggests that the energy density of cosmic rays increases from about 1 eV cm$^{-3}$ at the solar circle to about 6 eV cm$^{-3}$ at 4 kpc from the Galactic center. The interpretation of $\gamma$-ray data suggests similar numbers (e.g., Strong et al. 1996). However, these studies are severely hampered by the projection of emission along the line of sight. Long-wavelength radio astronomy offers the advantage of being able to measure actual path lengths, thereby greatly improving estimates of energy densities in the Galaxy. This is achieved by spatially resolving optically thick H II regions (very common at LWs) of known distance, against which the distributed synchrotron emissivity can be accurately determined (Kassim 1990). The power of this approach is the availability of relatively well-determined path lengths to the H II regions, allowing the true three-dimensional space distribution of cosmic-ray–induced synchrotron emissivities to be determined. A comparison of the local synchrotron emissivity with the known local energy density of cosmic rays would form the calibration needed to convert synchrotron emissivities to cosmic-ray energy densities.

Once the energy budget of cosmic rays is determined, then it is possible to critically compare the energetics of proposed cosmic-ray sources. For example, the supernova rate for our Galaxy is estimated to be about 1 per 30 yr. If a supernova produces $10^{51}$ ergs of kinetic energy, the average energy input rate is roughly $10^{42}$ erg s$^{-1}$. This number is comparable to the energy rate needed to maintain the Galactic cosmic rays (making specific assumptions about the poorly known energy density of cosmic rays in other parts of the Galaxy, e.g., Jones et al. 1998).

The above approach can be carried to external galaxies (which by virtue of their better perspectives minimize the "forest for the trees" problem associated with the Galaxy). Studies of SNRs in external galaxies, at cm wavelengths, have led to calculations of energy budgets showing that SNRs may in fact provide the needed energy (Duric et al. 1993; Duric et al. 1995; Gordon et al. 1998; Lacey 1998). However, these studies could be improved greatly at longer wavelengths. The above studies have found strong spatial correlations of SNRs with H II regions. Consequently, the thermal emission from the H II regions strongly contaminates the radio emission from the SNRs. The LWA, capable of $1''$ imaging and 1-mJy sensitivity at frequencies below 100 MHz, will allow the detection of SNRs even in the most confused regions of galaxies. The improved statistics would prove invaluable in gauging the role of SNRs in regulating the cosmic-ray production in external galaxies.

### *2.3.2 Supernova Remnants*

Supernova remnants, extended nonthermal emitting sources that are the principal sources of energy input into the ISM, are natural targets for study at LWs. Moreover, their often large angular sizes are well matched to the large FoV normally available at LWs. An excellent example is provided by Fig. 9, a wide-field image of the Galactic center made with the VLA at 330 MHz (Kassim et al. 1999). This image was used to discover the second closest known SNR to the Galactic center (Kassim and Frail 1996), and with this image a variety of other, previously unknown, nonthermal sources have been discovered in this extremely complex region. Long-wavelength studies of SNRs at high angular resolution and sensitivity should prove equally adept at finding new SNRs.

High-resolution, LW radio images will also serve to anchor spectral index studies of SNRs whose spatially resolved continuum spectra uniquely constrain the energy distributions of relativistic electrons. The key is to relate measured source spectral variations to dynamical structures, since models of particle acceleration in SNRs, either by shocks or by second-order Fermi (stochastic) acceleration in interior turbulence, predict structure in the particle distributions. Measured variations must be related to acceleration processes or the injection spectrum of the seed particles. Variations in older SNRs can also be related to compression of cosmic-ray gas and interstellar magnetic fields. Previous studies have had far too poor angular resolution at the longest wavelengths to explore such issues in detail, if at all.

Centimeter-wavelength studies of Cas A (Anderson and Rudnick 1996) have suggested that the spectrum of the emitting regions may be determined not only by current acceleration processes but also by the history of particle acceleration in the environment through which the particles have moved. Observations with the 74 and 330 MHz VLA systems have recently confirmed this surprising conclusion. Perhaps even more exciting has been the unique absorption measurements provided by the 74 MHz observations that reveal evidence for unshocked ejecta *within* Cas A, as predicted by theory (Kassim et al. 1995b). This measurement raises the prospect that many young supernova remnants may harbor cool thermal cores that the LW measurements can uniquely detect. The 74 MHz VLA system has also successfully detected thermal absorption from thermal filaments within the Crab nebula (Bietenholz et al. 1997). The detection of thermal absorption from within the first two SNRs observed with the new VLA system suggests that these effects may be common at LWs.

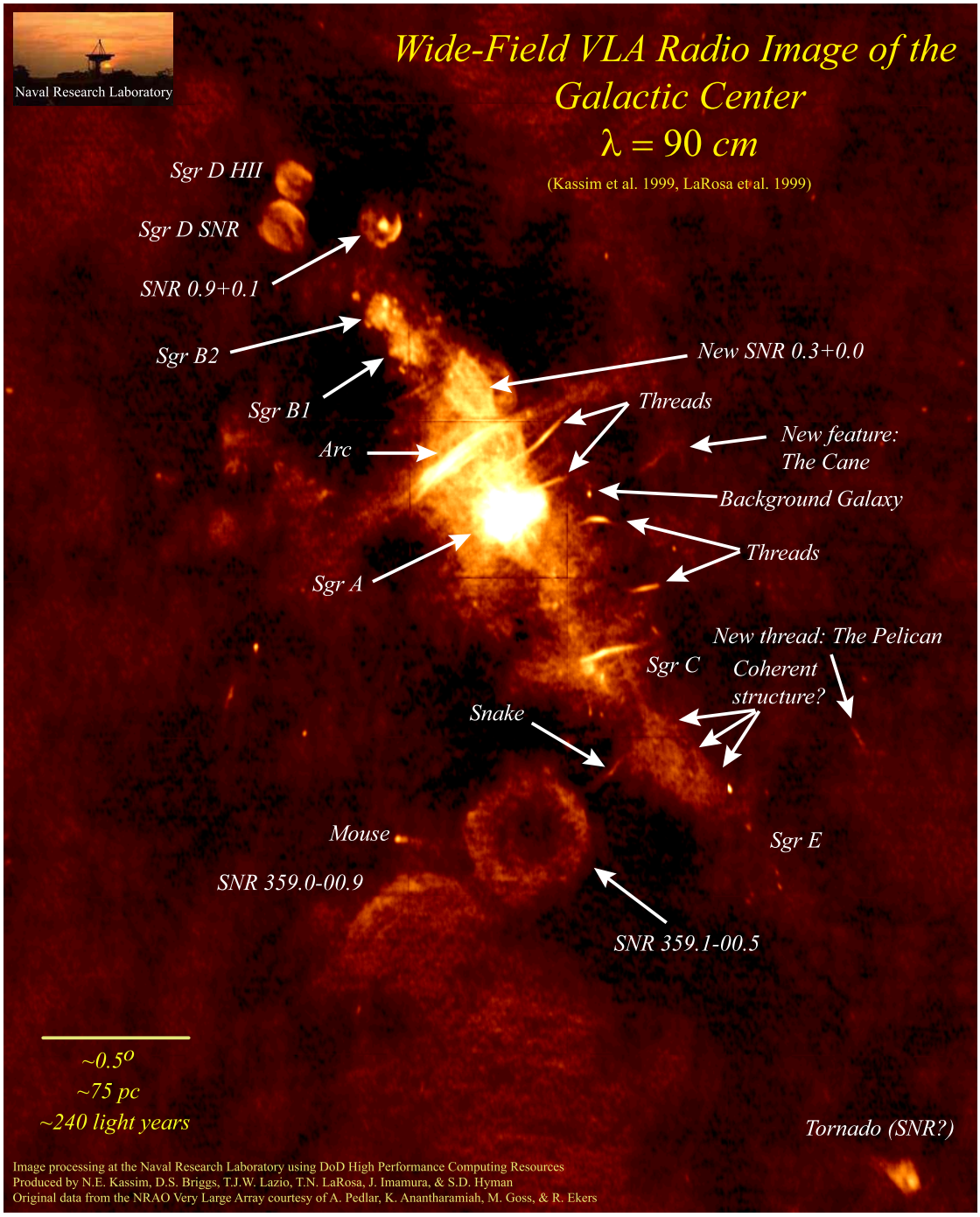


Fig. 9—A 330 MHz image of the Galactic center obtained with the VLA. This image covers $4^\circ \times 4^\circ$ at a resolution of $48'' \times 48''$. The rms noise level (excluding the bright sources on the Galactic ridge) is 5.9 mJy beam$^{-1}$.

In addition, useful information can be gained simply from the integrated LW spectra of SNRs. Predictions from Fermi-acceleration theory imply concave integrated spectra (i.e., hardening at higher frequencies) such as have been claimed in the case of the Tycho and Kepler's SNRs (Reynolds and Ellison 1992), but large error bars on the longest-wavelength measurements hamper these conclusions and restrict their extension to many more sources. Also, the Clark Lake 30 MHz studies of SNRs (Kassim 1989) were able to confirm and extend the original Culgoora 80 MHz SNR studies (Dulk and Slee 1975), which showed evidence of patchy foreground absorption by thermal gas in the ISM. More accurate, higher resolution measurements can extend such studies to many more objects and confirm whether the line-of-sight thermal absorption is indeed related to envelopes of normal H II regions as is currently speculated.

Sensitive LW observations should lead to the discovery of older, low–surface-brightness SNRs, which are known to be missing from catalogs due to severe selection effects (Green 1991). Discovery of such older SNRs, at the last stage of evolution before blending into the ISM, are potentially of great importance in discovering new pulsar-SNR associations and drawing links to unidentified $\gamma$-ray sources. Presently only the youngest pulsars can be associated with SNRs since remnants older than about $10^5$ yr have surface brightnesses too low for detection by current instruments.

The sensitivity and angular resolution of the LWA would extend these SNR studies to nearby external galaxies, increasing greatly the database. Recent statistical studies (e.g., birthrates, distribution, energetics) of complete, codistant samples of SNRs in nearby galaxies are proving extremely useful for exploring problems in stellar evolution, ISM structure, and for increasing sample sizes of poorly understood SNR subclasses (Duric et al. 1995; Jones et al. 1998). Sensitive, high-resolution, LW observations are required to complement existing higher frequency data by anchoring derived spectra, probing for ISM absorption effects (Wills et al. 1997), and to find new remnants.

### *2.3.3 H II Regions*

Observations at 330 MHz have demonstrated that measurements of optically thick H II regions can constrain source electron temperatures, emission measures, and filling factors (Kassim et al. 1989; Subrahmanyan and Goss 1996). At longer wavelengths these regions appear as cooler regions against a much hotter Galactic background, allowing kinematic distance ambiguities to be resolved and the superposition of thermal and nonthermal sources to be separated along complex lines of sight through the Galaxy.

A classic example is the 330 MHz VLA observation that revealed the thermal Galactic center source Sgr A West in absorption against the nonthermal-emitting Sgr A East supernova remnant (Pedlar et al. 1989), constraining the superposition of these sources along the most confused Galactic line of sight known. Observations with the 74 MHz VLA system promise to expand significantly the number of lines of sight on which this technique can be utilized, though a broadband system that can follow the onset of absorption at high angular resolution and as a function of frequency would make such studies far more powerful.

Kinematic-distance ambiguities resulting from radio-recombination-line measurements can be resolved using the detection, or nondetection, of H II regions in absorption below 100 MHz (Kassim 1990). On LWA maps, foreground ("near") H II regions would be much more prominent absorption features than distant ("far") ones.

### *2.3.4 Interstellar Propagation Effects*

All Galactic and extragalactic radio sources are observed after their radiation has propagated through the Galactic plasma. Variations in the plasma density produce refractive index fluctuations, scaling as $\nu^{-2}$, which in turn scatter the radiation. The magnitude of radio-wave scattering from the interstellar plasma is strongly direction dependent, but the effects can remain significant at frequencies of 10 GHz (Walker 1998) or higher (toward the Galactic center, Lazio and Cordes 1998). The density (refractive index) microstructure responsible for interstellar scattering occurs on scales of order 1 AU. The density fluctuations, in turn, are thought to arise from velocity and/or magnetic field fluctuations. In addition to their corrupting effects, interstellar propagation effects are a powerful sub-parsec probe of the interstellar plasma, can provide a tracer of energy input into the ISM, and may be linked to cosmic ray propagation (Section 2.3.1).

Long-wavelength observations of compact sources provide a powerful diagnostic of propagation effects from the ISM. The scatter-broadened angular diameter of a compact nonthermal source scales as $\lambda^2$, while the resolution of a telescope and the minimum apparent size constrained by synchrotron self-absorption both scale as $\lambda$. Thus, interstellar scattering studies are optimized with high-resolution, LW observations.

The LWA would prove useful for interstellar scattering studies in two respects. First, it would simply increase the number of lines of sight on which scattering observations could be conducted. The most recent compilation of scattering observations contained 223 sources (Taylor and Cordes 1993). The LWA could increase the number of known pulsars by a large amount (Section 2.5.1). Scattering observations can also be exploited to select sources at various distances. For instance, pulsars in and beyond the Galactic center would be resolved out by the LWA (Cordes and Lazio 1997), but pulsars in the inner Galaxy between us and the Galactic center (e.g., in the molecular ring) will still be detectable. The vast majority of scattering studies, however, have been conducted using compact extragalactic sources viewed through regions of intense scattering (e.g., Cygnus, Spangler and Cordes 1998; the Galactic center, Frail et al. 1994; Yusef-Zadeh et al. 1994), where the scattering effects can be detected at frequencies near 1 GHz on baselines of length 50 to 5000 km. Figure 10 illustrates this bias toward regions of intense scattering. Because of the $\lambda^2$ scattering dependence vs. the $\lambda$ synchrotron–self-absorption–size dependence, the LWA would enable studies of the density and field microstructure in less intense scattering regions, such as those near the Sun.

Second, the LWA could be expected to contribute to a better understanding of the generation of the probably turbulent density fluctuations, their distribution in the Galaxy, as well as the detection of some novel effects that probably cannot be detected at higher frequencies.

#### 2.3.4.1 Density Fluctuation Genesis

Current shock-acceleration theories (Ellison et al. 1994), relevant to the origin of cosmic rays, also suggest that upstream of a SNR should be an ideal site for the generation of the density fluctuations responsible for interstellar scattering. High-frequency searches for the signatures of such upstream turbulence have a mixed record (Spangler et al. 1986). The $\lambda^2$ dependence of interstellar scattering would allow much more stringent tests to be applied.

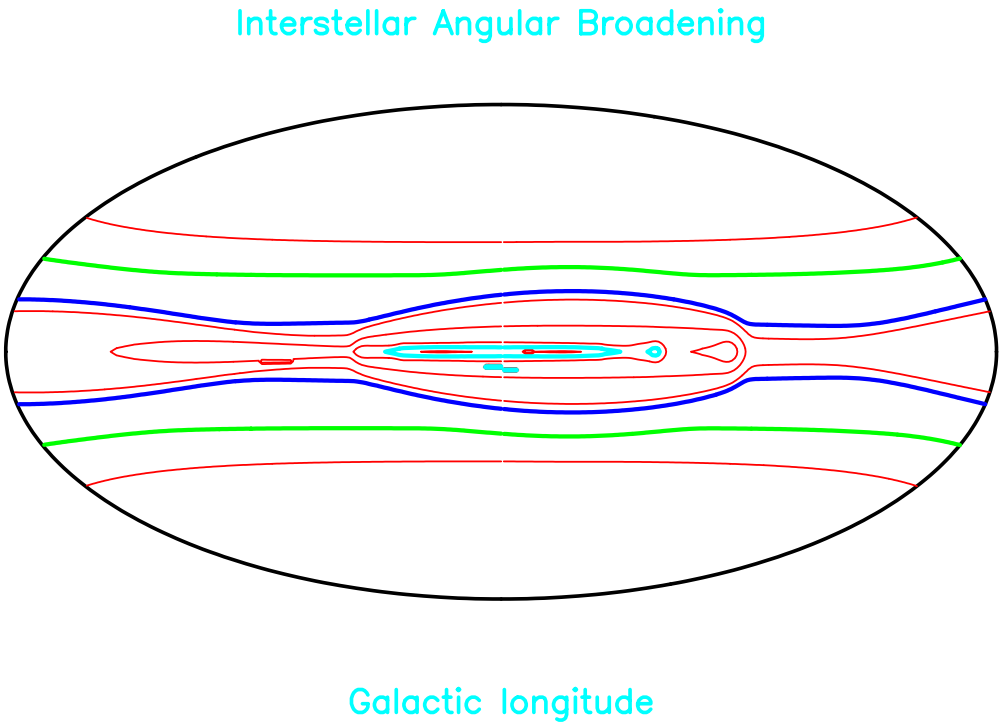


Fig. 10—The Galactic distribution of interstellar scattering. The thin red lines are contours of constant angular broadening diameter as calculated from the Taylor-Cordes model (Taylor and Cordes 1993) at 1 GHz. The Galactic center is at the center of the figure and Galactic longitude increases to the left. The heavy cyan line delineates the regions of scattering accessible to an interferometer with 30 km baselines operating at 74 MHz (e.g., VLA). The heavy blue line delineates the regions of scattering accessible to an interferometer with 8000 km baselines operating at 330 MHz (e.g., VLBA). The heavy green line delineates the regions of scattering accessible to an interferometer with 500 km baselines operating at 20 MHz (e.g., LWA). This model does not account for a few lines of intense scattering, so localized regions of intense scattering may exist outside of these nominal limits that could be studied by these instruments.

#### 2.3.4.2 Galactic $z$-Distribution of Scattering

Ionized gas is found several kiloparsecs above the Galactic plane (the "Reynolds layer"). The scale height of the density fluctuations responsible for interstellar scattering is about 1 kpc, inferred from observations of high-latitude pulsars (particularly those in globular clusters) and LW interplanetary scintillation measurements. The agents presumed to be responsible for generating density fluctuations—SNRs and H II regions—have a much smaller scale height ($\sim 0.1$ kpc). As Fig. 10 illustrates, the LWA could probe to higher latitudes than existing instruments and would provide additional information about the vertical distribution of the scattering material and clues about any other agents responsible for generating the density fluctuations. Particularly valuable would be deviations from the smooth distribution of scattering material predicted by current models (Taylor and Cordes 1993).

#### 2.3.4.3 Three-Dimensional Distribution of Scattering

The magnitude of scattering observables, e.g., angular broadening, depends not only upon the total rms electron density fluctuations toward a source, but also upon their distribution along the line of sight. For instance, angular broadening is more pronounced the closer the scattering medium is to the observer. Thus a comparison of the amount of angular broadening along similar lines of sight to a Galactic and extragalactic source can reveal the *radial* distribution of the scattering medium (Moran et al. 1990; Lazio and Cordes 1998). Furthermore, different scattering observables have different radial dependences. For instance, consider a pulsar at a distance $D$ and a localized region of scattering at a distance $x$ with $0 \leq x \leq D$ and $s \equiv x/D$. Then the magnitude of pulse broadening depends upon the distribution of scattering weighted by $s(1-s)$ while angular broadening is weighted by $s^2$(Cordes and Rickett 1998). Thus, a comparison of scattering observables toward the same object can also reveal the *radial* distribution of scattering toward that object. High-frequency observations have shown, perhaps not surprisingly, that scattering toward the Crab pulsar is dominated by the Crab Nebula (Gwinn et al. 1993). The LWA could extend such studies to a much larger number of pulsars, allowing the local *three-dimensional* distribution of scattering to be mapped.

#### 2.3.4.4 Spatially Limited Scattering

The density fluctuations responsible for interstellar scattering have a spatial spectrum. The largest scale on which these density fluctuations occur is about 1 pc near the Sun and may be of the order of 0.01 pc in regions of intense scattering; this scale is presumably related to the injection of energy into the ISM that produces the density fluctuations. At LWs, the angular extent of the scattering region may be less than the nominal scatter-broadened angular diameter of a background source. If so, the shape of the scatter-broadened image may be affected by the fact that the scattering is occurring only in a limited volume (Cordes 1990). The orientation and distortion of the image would then provide information about the volume in which the scattering was occurring.

### *2.3.5 Carbon Recombination Lines*

As interstellar carbon ions recombine into very high Rydberg states (up to $n = 768$), absorption lines below 150 MHz are generated. The carbon atoms in these high states are very sensitive to the

interstellar environment and permit excellent measurements of density, temperature, and ionization levels to be carried out (Payne et al. 1994). A number of Galactic regions that produce these lines have been found, including a large region that stretches 40° along the Galactic plane in the central region of the Galaxy (Erickson et al. 1995). Until now, all observations of these lines have been made with filled apertures with extremely low angular resolutions. The very central portion of the LWA should have sufficient surface-brightness sensitivity for detection of these lines and would provide much needed angular resolution to map their distribution. The sensitivity of the LWA would be sufficient not only to increase the number of such regions studied in the Galaxy, but also would allow these studies to be extended to external galaxies.

## 2.4 Solar System Science

### *2.4.1 Solar Radar*

There is at present great interest in developing a means of detecting and predicting the arrival times of *Earthward-directed* CMEs, the main cause of increasingly costly geomagnetic storms. Currently, the best way of studying CMEs has been from space, which is expensive and often unreliable. Furthermore, as Fig. 11 illustrates, space-based coronographs are not well suited for studying Earthward-bound CMEs. A revolutionary ground-based technique of detecting and tracking CMEs with long-wavelength solar radar is now being considered, and the LWA would be an ideal imaging receiver for such experiments.

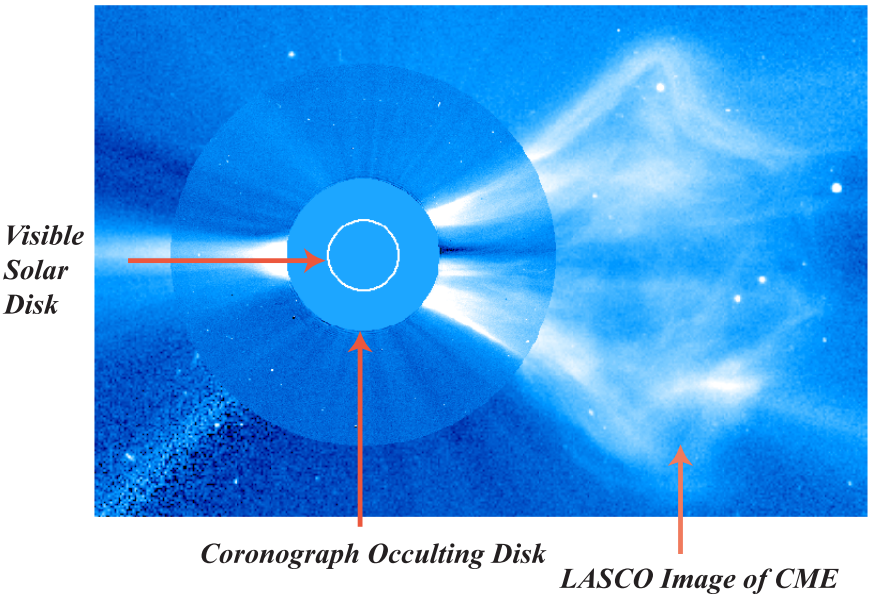


Fig. 11—A LASCO coronograph image of a transversely directed CME. Coronograph images are most effective for determining transverse motions of CMEs. Figure courtesy of NRL, Code 7600.

The El Campo radar, built by the Lincoln Laboratory, detected 38 MHz radar echoes from the Sun for a period of 9 years in the 1960's (James 1968, 1970). Huge, rapidly moving "targets" were occasionally observed but this was before the space-borne coronagraph discovery of CMEs

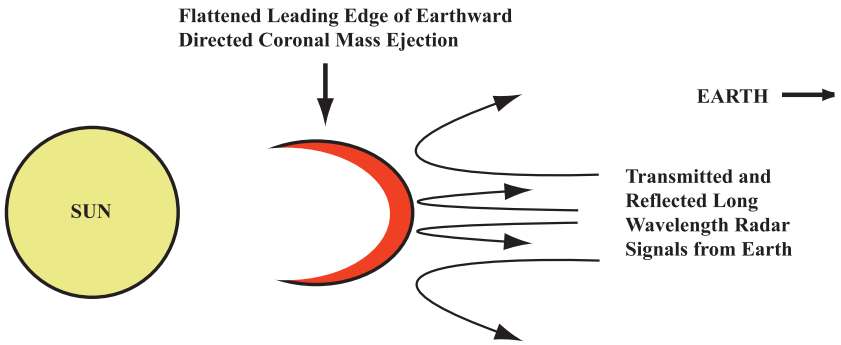


Fig. 12—Basic geometry of solar radar. Long-wavelength signals transmitted from Earth in the 10 to 80 MHz range will be reflected off the solar corona at an altitude corresponding to the relevant plasma frequency. An outward moving CME will impose a Doppler-shifted signature on the reflected signal that can be used to detect and image the CME.

(Gosling et al. 1974), and the physical nature of these "targets" was a mystery. It is now thought that CMEs were being observed.

The reliable detection and monitoring of CMEs is of great practical importance. CMEs that impact the Earth's magnetosphere can result in hundreds of millions of dollars in damage to spacecraft, communication, and electrical power systems. A LW transmitter coupled with a high–angular-resolution receiving array would form an extremely cost-effective system to detect and track CMEs.

Rodriguez (1996) has summarized the potential of 10 to 80 MHz radar systems for detecting CMEs; Fig. 12 illustrates the basic principle. The Doppler shift introduced by different parts of an outward-moving CME will result in a characteristic frequency- and time-dependent signature in the reflected signal. The rich information inherent in this measurement could open an entirely new window on CME studies, yielding their angular distribution, ranges, and line-of-sight velocities. Figure 13 shows that combining the radial velocity obtained from the Doppler shift with the transverse velocity obtained from imaging is required to determine the CME total velocity vector. This would allow for accurate predictions of CME Earth-arrival times. Sufficient transmitting facilities now exist (e.g., Arecibo Observatory, over-the-horizon radars that are no longer required for military purposes), but adequate receiving facilities are needed for such a project.

Currently, space-based coronographs are used to detect and track CMEs (Fig. 11). However, space-borne white-light coronagraphs detect the Thomson-scattered light from the CME material and therefore are less sensitive to structures propagating at large angles out of the plane of the sky, such as Earth-directed CMEs. An array of coronographs in the Earth's orbit could provide the stereoscopic view to determine this information, but at significant cost and a limited, somewhat unpredictable lifetime. A cheaper and more reliable LW radar system (incorporating the LWA as its imaging receiver) offers a great cost advantage over such space-based CME monitoring schemes.

Aside from the macroscopic physics of direct interest to the space weather program, there is great potential in unraveling the microscopic physics of the solar radar scattering mechanism.

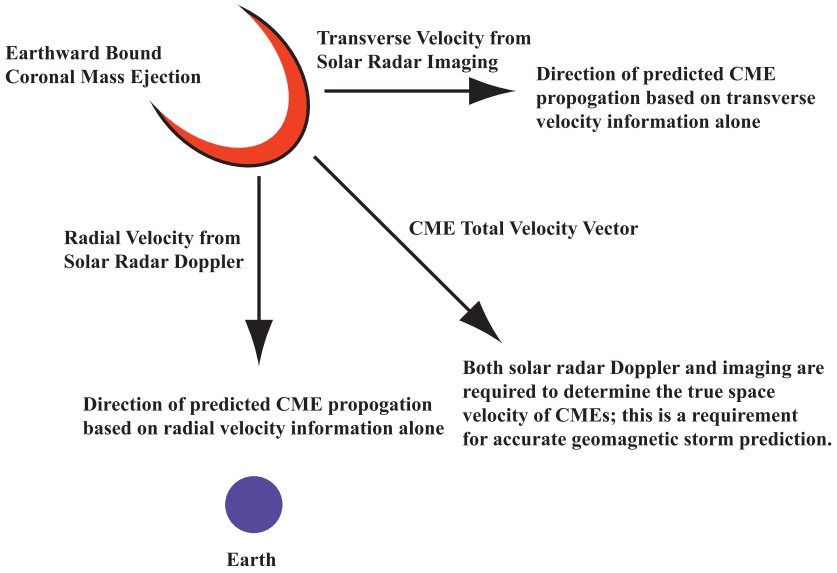


Fig. 13—A schematic illustrating that both Doppler-determined radial velocities and transverse velocities acquired from imaging are required to determine accurately the Earth arrival time of a CME. With a typical velocity of 200 to 800 km $s^{-1}$, a typical CME requires about three days to reach Earth after its formation at the Sun.

An understanding of this mechanism is key to solving the puzzles of the spectral shape, the large Doppler spread, the Doppler shift, and the variation in solar radar cross section. Various mechanisms have been suggested, including turbulence in the local medium (Kundu 1965), fluctuations in the altitude of the plasma resonance level due to electron density fluctuations in the solar wind (Ishimaru and Woo 1978), ion acoustic waves (Gordon 1968), and coherent lower hybrid waves (Wentzel 1981). The possibility of coherent coronal plasma waves is especially intriguing as it is a topic of current interest, and a search for such waves was included in the observing program for the Solar and Heliospheric Observatory (SOHO) spacecraft (DeForest 1996).

Once the microphysics is understood, solar radar could become a probe of the solar plasma on a par with the modern coherent and incoherent radars used to probe Earth's ionosphere. In particular, the astonishingly accurate plasma physical theory of incoherent scatter radar has allowed a detailed and productive study of our nearest space plasma in a way undreamed of before its discovery. A similar scientific potential may be hidden in the coronal scattering mechanism.

If the LWA were located at the VLA site, Arecibo Observatory would provide an excellent location for a transmitter to conduct bistatic solar radar experiments. The National Astronomy and Ionosphere Center conducted solar radar observations in the 1960s (Parrish 1968) and has assisted in developing a preliminary engineering design for a frequency agile solar radar transmitter, illustrated in Fig. 14, which would upgrade Arecibo with the transmitting power required to conduct bistatic imaging solar radar studies with the LWA located in the southwestern United States.

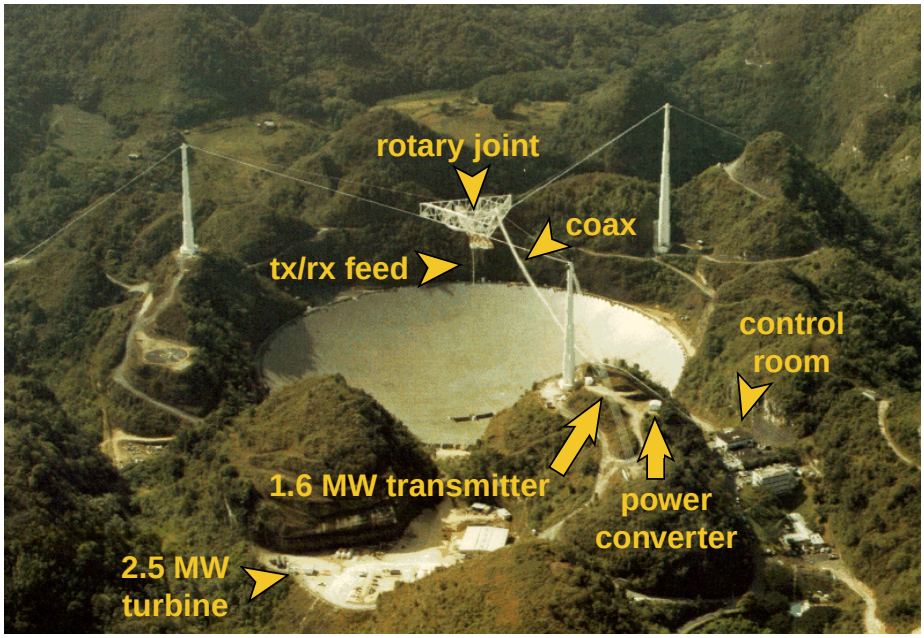


Fig. 14—Key elements of an imaging solar radar transmitter at Arecibo. Transmitter power would be 1.6 MW CW with an antenna gain of 38.2 dBi at 46.8 MHz. Bistatic Arecibo-LWA imaging solar radar observations would be possible for a period of up to 2.6 hr centered on local (Arecibo) noon for a southwestern US LWA location.

### *2.4.2 Solar Science*

The central portion of the LWA would make an excellent multifrequency radioheliograph that could be used to continue the solar observations pioneered by the Culgoora and Clark Lake radio telescopes in the 1970s and 1980s. The decommissioning of these instruments has severely handicapped solar radio astronomy. At present, there is no solar–radio-imaging capability at frequencies below roughly 150 MHz anywhere in the world. Also, there is only one radioheliograph (Meudon, France) that can provide simultaneous spectral and (limited) spatial information for frequencies 160 to 600 MHz. Observations with the central portions of the LWA could provide important insight in the physics of the solar corona, such as:

- Recent results from joint radio–white-light observations (e.g., Maia et al. 1999) suggest that LW radio observations can provide unique information on the initial CME stages, such as the coronal structures involved, speeds, densities, and the sites of particle acceleration.
- In the past, instrument sensitivity has prevented reliable imaging of the quiet solar corona at LWs. LWA solar maps will permit high quality density measurements of various coronal structures (e.g., streamers) and the monitoring of the long term variability of the outer corona.
- The improved resolution and sensitivity of the LWA could allow imaging of certain structures within the CME itself (e.g., plasmoids, moving Type IV bursts). With the help of the radio spectrum, one can derive the magnetic field in these structures. Such information is crucial in

understanding the development and subsequent propagation of CMEs but has been sketchy or missing altogether so far.

- The LWA will be able to study Type III bursts in the outer corona in detail and at a level of sensitivity far greater than in the past. This should shed light on energy release in the outer corona. The LWA will also be able to study Type II radio bursts, which are driven by magnetohydrodynamic shocks, further elucidating the relationship between coronal shocks and interplanetary shocks.
- The combination of the LWA with spaced-based solar radio instruments that operate at longer wavelengths than the LWA (e.g., WIND/WAVES, Ulysses, STEREO) will permit the thorough study of the propagation of coronal material through the interplanetary medium to the Earth, which can contribute not only to solar but to the magnetospheric physics as well.

In addition to providing detailed observations of solar nonthermal emission at unprecedented angular resolution, scattering measurements towards background sources offer an excellent opportunity to study the structure of turbulence in the solar corona and interplanetary medium. Previous occultation studies below 100 MHz have been limited to using the Crab pulsar as a background source. The LWA should provide access to hundreds or even thousands of background sources with which to probe the solar corona and foreground heliosphere on a routine basis as well as achieve the angular resolution required to properly complement higher frequency (e.g., 330 MHz VLA) studies.

## 2.5 Coherent Emission Sources

High–brightness-temperature emission at long wavelengths is widely assumed to result from coherent emission processes. The Sun, Earth, Jupiter, and pulsars are good examples of objects that radiate via such processes. Coherent emission occurs most readily at long wavelengths because the size of the region from which coherent emission occurs must be smaller than the wavelength—long wavelengths allow for large regions and large numbers of particles. Plasma processes seem a natural means of producing coherent radiation. If so, coherent radiation is intimately coupled to the magnetoionic parameters of the emitting plasma—the plasma frequency, the gyrofrequency, and the collision frequency—and carries a wealth of information concerning the structure of the plasma source. In addition to known sources of coherent emission discussed below, the LWA may also identify new classes of coherent emitters, such as cyclotron maser emission from extrasolar planets (Dulk et al. 1997; Farrell et al. 1999).

### *2.5.1 Pulsars*

Pulsars were discovered using a LW instrument (81 MHz, Hewish et al. 1968), and most searches for radio pulsars to date have searched for dispersed, pulsed emission at frequencies of 400 to 1400 MHz. Alternate search techniques will need to be employed at longer wavelengths, as pulse broadening from interstellar scattering will become increasingly important. At 100 MHz, only nearby pulsars—those with dispersion measures DM less than or equal to 100 pc $cm^{-3}$—will suffer pulse broadening less than 1 s and be seen as sources of pulsed emission; at 30 MHz, only a handful of the very nearest pulsars, DM less than or equal to 10 pc $cm^{-3}$, will be seen as sources of pulsed emission (Cordes 1990).

The LWA could serve as a useful pulsar search instrument by searching for sources having pulsar-like characteristics, other than pulsed emission. Since pulsars generally, and millisecond pulsars in particular, have steep spectra, compact steep-spectrum sources would be excellent candidates for deep, higher-frequency periodicity searches. The prototypes of this search technique were the Clark Lake Radio Observatory observations of 4C21.53 and M28, which ultimately led to the identification of the first known millisecond pulsars (Erickson and Mahoney 1985; Mahoney and Erickson 1985; Figs. 15 and 16). More recently, Navarro et al. (1995) discovered the millisecond pulsar PSR J0218+4232 using similar techniques. A search for compact steep-spectrum sources would also be less likely to select against the following classes of pulsars: distant, highly scattered pulsars (Lazio and Cordes 2001); submillisecond pulsars; and pulsars in tight binaries—objects for which there have been serious selection effects in most existing surveys.

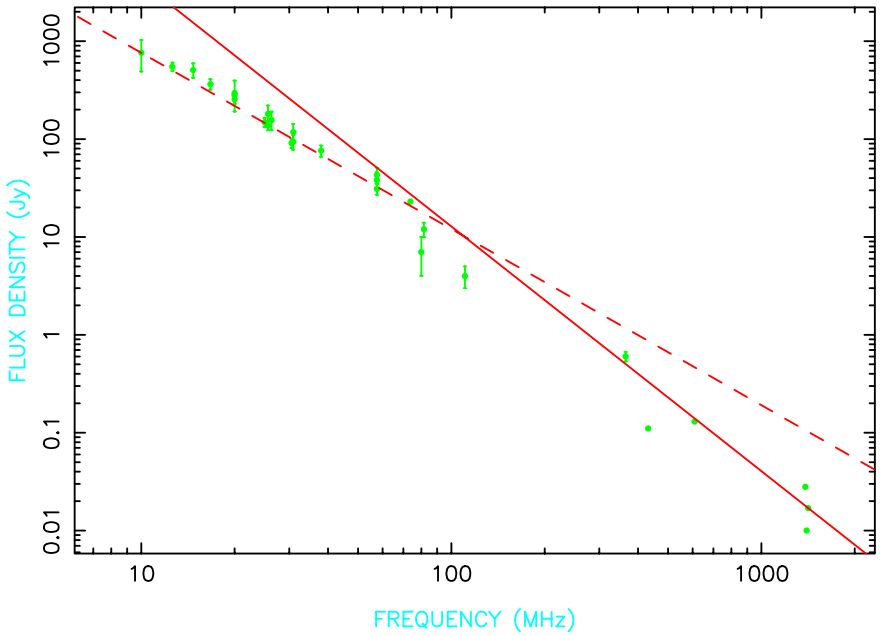


Fig. 15—The low-frequency spectrum of the millisecond pulsar PSR B1937+21. Data are from Erickson and Mahoney (1985). The solid line shows a spectrum with a spectral index of $-2.5$, and the dashed line shows a spectrum with a spectral index of $-1.8$.

Current design goals for the LWA are that it would be capable of detecting pulsars with 80 MHz peak flux densities of 5 mJy, assuming a 10% duty cycle. [For comparison, a recent 80 MHz *periodicity* survey by Shrauner et al. (1998) had a sensitivity of 200 mJy.] The equivalent 400 MHz flux-density sensitivity, assuming a typical pulsar spectrum of $-1.6$, is 0.4 mJy, approximately an order of magnitude better than the recent Parkes southern-hemisphere pulsar survey (Manchester et al. 1996; Lyne et al. 1998), which found a total of 100 previously unknown pulsars. The pulsar luminosity function[1] is $dN/d(\log L) \propto L^{\beta}$ with $\beta \approx -1$. Thus, we anticipate that a survey with the LWA could increase the number of known pulsars by 500 to 1000—an increase of 50 to 100%.

[1]The luminosity is $L_{400} = S_{400}D^2$, where $S_{400}$ is the 400 MHz flux density in mJy and $D$ is the distance in kpc.

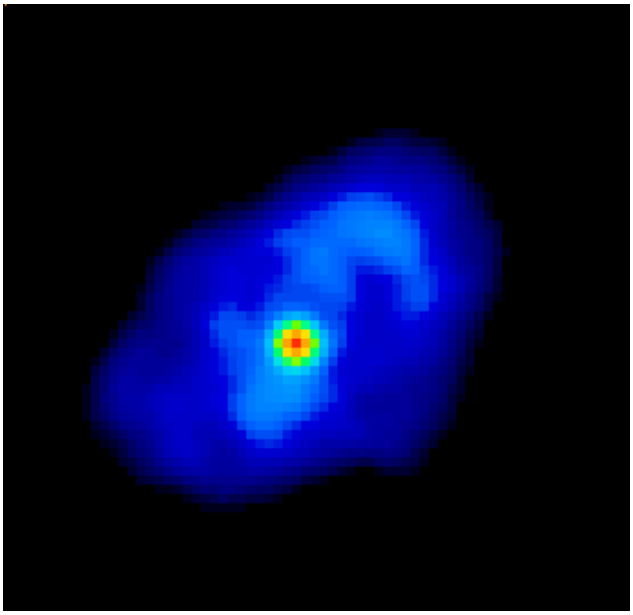

Fig. 16—The Crab Nebula and pulsar at 74 MHz

The estimate of the number of pulsars that could be detected by the LWA (as well as the estimate of the total number in the Galaxy) is affected by the faint end of the luminosity function. There are indications that this luminosity function begins to turn over in the range 0.3 to 1 mJy kpc$^2$ (Dewey et al. 1985; Lyne et al. 1998), though current pulsar surveys also become incomplete near luminosities of 10 mJy kpc$^2$ (see also Tauris et al. 1994). The LWA's ability to detect faint pulsars would aid in assessing the extent to which this low-luminosity turnover is real.

The design of the LWA is also ambitious enough that it would probably be sensitive to pulsars in nearby galaxies. For instance, pulsars with luminosities in excess of $10^2$ mJy kpc$^2$ (and spectral indices of $-1.6$) would have 100 MHz flux densities of 1 mJy at the distance of M31. [Within 1.5 kpc of the Sun, Lyne et al. (1998) find about ten pulsars that are bright enough.] For comparison, only a handful of pulsars are currently known outside the Galaxy, and these are in the Large and Small Magellanic Clouds (distance $\approx 0.05$ Mpc).

The presence or absence of LW emission from pulsars can also serve as a powerful constraint on models of the pulse emission process. A recent example has been the claimed detection of pulsed emission from the 237 ms gamma-ray pulsar Geminga at frequencies between 40 and 100 MHz (Kuz'min and Losovskii 1997a; Kuz'min and Losovskii 1997b; Malofeev and Malov 1997; Shitov et al. 1997; Shitov and Pugachev 1997; Vats et al. 1997). Subsequent attempts to confirm these claims have not been successful (35 MHz, Ramachandran et al. 1998; 74 MHz, Kassim and Lazio 1999). Nonetheless, the discovery of a pulsar that radiated strongly at frequencies $\nu \approx 100$ MHz but not at higher frequencies could provide an example of a nearly aligned rotator whose emission mechanisms are different than those of the typical pulsar (Gil et al. 1998; Malov 1998).

### *2.5.2 Extrasolar Planets*

Jupiter emits intense, coherent bursts of radiation at decameter wavelengths (Carr and Wang 1990), and its thermal emission has been detected recently with the VLA 74 MHz system (de Pater 1999). It has often been suggested that Jupiter-like planets orbiting other stars might be detectable by decametric observations of similar emission. Such planets, however, would have to radiate at levels several orders of magnitude greater than Jupiter in order to be detectable. At a distance of 10 pc, Jupiter's bursts would be at the 10 $\mu$Jy level.

The Jupiter-like extrasolar planets that have recently been identified are generally larger and closer to their stars than Jupiter, making it likely that they may also be considerably more active in the decametric wavelength regime. Schaefer et al. (1999) have proposed that Jovian planets close to their primary may produce an RS CVn-like phenomenon in which the magnetic fields of the star and planet would become tangled. Reconnection events would then accelerate particles producing LW radio emission. In support of this model, they have identified nine solar-type stars that have been observed to undergo optical flares with energies of $10^2$ to $10^7$ times larger than those on the Sun.

An alternate mechanism would be cyclotron-maser emission from extrasolar planets. Farrell et al. (1999) recently estimated coherent cyclotron emission levels from extrasolar planets using scaling laws for the strength of planetary magnetic fields and radio emission for the planets in our own solar system. In our solar system, planets with substantial magnetic fields are also in continuous interaction with the local solar wind, which efficiently creates electric currents at their magnetospheric boundaries. These current ultimately deposit a portion of their energy in the auroral region, thereby generating the visible aurora and auroral radio emission. At Earth, Jupiter, and Saturn, the cyclotron emission level is strongly correlated with the character of the solar wind.

In the power estimates of the cyclotron radiation from extrasolar planets, it was assumed that there is an analogous stellar wind-magnetospheric interaction. The radio power from a planet orbiting a Sun-like star will then scale as

$$P \sim w^{0.8} M^{1.3} d^{-1.6}, \tag{1}$$

where $w$ is the planetary rotation period, $M$ is the planet mass, and $d$ is the star-planet distance. Table 3 summarizes the expected flux levels from a number of known extrasolar planets. The estimates indicate that the best candidate for detection by the LWA of solar wind-driven cyclotron emission is $\tau$ Bootes, with an expected median amplitude of about 2 mJy at 28 MHz, an intensity level many decades below the current limit of detectability. However, planetary radio sources are exponential amplifiers, and arithmetic increases in stellar wind speeds correspondingly increase power levels geometrically. Thus, in extreme conditions, the estimates for extrasolar sources could be a factor of 100 to 1000 times higher, becoming closer to a detectable level even with current equipment.

Detection of such cyclotron emission would allow constraints to be placed on various parameters of the planet, such as the strength of its magnetic field and the presence of any close, large satellites. A search for cyclotron-maser emission at 330 MHz has been conducted (Dulk et al. 1997), and a search using the new 74 MHz VLA system is underway. The increased sensitivity of the LWA would increase the possibilities of detecting any such planets and improve constraints inferred from such detections.

Table 3—Estimated Cyclotron Maser Emission Levels from Extrasolar Planets

| Star | Frequency Range of Emission (MHz) | Flux Density (mJy) |
|---|---|---|
| 51 Peg | 0.2–2 | 0.039–390 |
| $\nu$ And | 0.3–3 | 0.024–240 |
| 55 Cnc | 0.1–1.6 | 0.015–150 |
| $\rho$ CrB | 8–77 | 0.0013–13 |
| 16 Cyg B | 15–140 | $3 \times 10^{-5}$–0.3 |
| 47 UMa | 42–403 | $4 \times 10^{-5}$–0.4 |
| $\tau$ Boo | 9–84 | 0.22–220 |
| 70 Vig | 175–1700 | $2.3 \times 10^{-4}$–2.3 |
| HD 114762 | 351–3400 | $1.5 \times 10^{-4}$–1.5 |

### 2.6 Surveys and Serendipitous Discoveries

Most existing radio sky surveys have been made at relatively LWs (e.g., the Cambridge surveys). From these surveys come both serendipitous discoveries (e.g., pulsars) and the catalogues of sources used for high-resolution mapping at high frequencies. Serendipitous discoveries often provide the greatest opportunities for advances in our understanding of the physics of astronomical objects. An excellent recent example is the 6C survey discovery of the extraordinary jet in NGC6251. The LWA would be an excellent survey instrument that can be "expected" to uncover unexpected classes of objects. The array's sensitivity will be sufficient to allow source number counts at decametric frequencies where synchrotron aging is negligible but where cosmological tests have not yet been attempted. The capability to image a large field quickly and at high angular resolution and sensitivity would allow for efficient studies of variable and transient radio source populations, for example at the Galactic center (Zhao et al. 1992).

## 3. LONG WAVELENGTH ARRAY CONCEPT

### 3.1 Astrophysically Driven Array Properties

#### *3.1.1 Frequency Range*

Frequency versatile LW observations are powerful diagnostics of emission, absorption, and scattering phenomena. For emission the instrument can provide superior point-source and surface-brightness sensitivity to steep-spectrum sources, accurately constraining emission spectra. This drives the observing frequencies to the limit allowed by the ionosphere. A few existing instruments can make measurements to just above the LW range (e.g., Cambridge and GMRT at 151 MHz, the VLA and Westerbork at 330 MHz) but only the VLA at 74 MHz and the GMRT at 50 MHz will provide imaging capabilities at LWs. (The GMRT's angular resolution will be a few arc-minutes, well above that planned for the LWA.)

The case of absorption is perhaps more interesting. Here, the interaction of nonthermal emitting sources with absorbing thermal material allows unique observations for probing the distribution of both the emitters and absorbers. The case of constraining cosmic-ray properties by measuring the foreground emission along lines of sight to absorbing H II regions has already been discussed. Furthermore, LW observations are key to studying intrinsic self-absorption processes, such as synchrotron self-absorption in compact extragalactic sources. The key here is that all of these absorption effects are best studied at frequencies below 100 MHz where the observable properties of the radio universe acquire a completely different character because of absorption effects.

These scientific considerations direct us to as long a wavelength as possible above the ionospheric absorption cutoff near 20 m (10 MHz). However, past experience has also taught us that ionospheric scintillations, which cannot be removed by self-calibration, will degrade a non-negligible fraction of the data below roughly 30 MHz. Thus, we plan for an instrument that can reach 15 MHz, with a realization that it will operate with reduced efficiency below 30 MHz.

#### *3.1.2 Frequency Versatility*

In addition to the need to go to frequencies below 150 MHz, the rapid variation in the contrast between emitting and absorbing regions as a function of frequency drives the desire for a broadband instrument. For example, the ability to constrain the physical properties of a source exhibiting synchrotron self-absorption is significantly enhanced if one can provide several points on the LW spectrum. Thus, we desire an instrument whose response is sufficiently broadband to extend from approximately 150 MHz through the lower limit of 15 MHz discussed above. This suggests the use of frequency-independent, log-periodic antennas.

#### *3.1.3 Angular Resolution and Array Size*

Poor angular resolution is the single greatest limitation that has reduced the scientific yield of previous LW instruments. In general, observations below 100 MHz have been limited to angular resolutions of tens of minutes of arc or more. This is not sufficient to resolve most of the interesting structures. Hence sub-arcminute resolution would open up a completely new window on this region of the electromagnetic spectrum. Experience from LW VLBI measurements shows that very few sources exhibit compact structure that can be detected with reasonable sensitivities on baselines longer than 500 km. Thus, a reasonable goal would be an array whose longest dimensions were approximately 500 km, rendering approximately $8''$ and $0.8''$ resolution at 15 and 150 MHz, respectively. This nicely places the maximum resolution at the longer wavelengths just above the natural limit set by interstellar and interplanetary scattering ($\sim 5''$ at 15 MHz; Weiler 1990).

### 3.2 Technical Considerations

The new NRL-NRAO 74 MHz observing system at the VLA is the first to break the "ionospheric barrier" successfully and demonstrates that interferometry at LWs can now be extended to baselines far longer than the 3-km scale previously thought to be dictated by the ionosphere. In Section 3.3, we capitalize on this breakthrough and present our proposal for the LWA, a much larger and broadband instrument that could tackle the many interesting scientific problems outlined above. Here, we discuss critical calibration and imaging issues unique to this type of instrument, and we extend the results developed by Perley and Erickson (1984) in their initial consideration of

a 74 MHz system for the VLA. Extensive simulations are required to confirm these approximations and drive the detailed design of any much larger system.

### *3.2.1 Field of View*

The phase fluctuations introduced by the ionosphere can be tracked by self-calibration as time-variable contributions to the antenna-based phase solutions. However if the FoV is larger than the "isoplanatic patch," then the time variable ionospheric phases take on a positional dependence as well. New imaging algorithms (e.g., in `aips++`) address this problem and are needed for the 74 MHz VLA where the FoV (greater than 10°) exceeds the isoplanatic patch size (greater than 5°). However, the LWA would better limit the FoV through hardware design. This can be achieved by phasing the signals from closely spaced dipole antenna "elements" into a single antenna "bank." One bank would be analogous to an individual VLA antenna, and if made large enough would limit the FoV; for example, the Clark Lake TPT array (Erickson et al. 1982) FoV at 74 MHz was less than 2.5°, a result of its large antenna banks. Additional constraints on the FoV are provided by bandwidth and time averaging effects.

### *3.2.2 Sensitivity*

Sensitivity issues at long wavelengths are unique. Two important characteristics are that the system temperature (i.e., thermal noise) is dominated by the sky brightness, and that confusion from background sources is significant. Perley and Erickson (1984) explored these issues for the 74 MHz VLA, and here we present results of that study modified for the much larger LWA proposed in Section 3.3.

The thermal noise contributed by the Galactic background scales as $\nu^{-0.55}$. For directions away from the plane, the equivalent system thermal noise on an individual baseline, $S_{\rm thermal}$ is

$$S_{\rm thermal} = 50\,{\rm Jy}\left(\frac{408}{\nu}\right)^{2.55}\left(A_{\rm eff}\sqrt{t\Delta\nu}\right)^{-1}. \quad (1)$$

Here $\nu$ is the observing frequency in MHz, $A_{\rm eff}$ is the collecting area of an individual antenna (or bank of dipoles as described above) in m$^2$, $\Delta\nu$ is the receiver bandwidth in MHz, and $t$ is the integration time in seconds. The confusion noise arises from the contribution to the system temperature from unmodeled sources in the FoV (main beam confusion) and background sources rumbling through the sidelobes (sidelobe confusion). Extending the results of the random-walk analysis presented by Perley and Erickson (1984) to the case of a 200 km baseline, the equivalent system confusion noise is given by

$$S_{\rm confusion} = 6.6\,{\rm Jy}\left(\frac{408}{\nu}\right)^{0.75}(\nu t\Delta\nu)^{-1/2}. \quad (2)$$

This expression assumes that 50% of the flux in the main FoV can be reasonably modeled. Table 4 shows that this is always a good assumption. The first column is $f$, the fraction of the total flux in a 1° FoV at 74 MHz that is available for modeling. The second column $S_{\rm mod}$ shows the total flux in the model, indicating that a typical 1° field will contain 9.8 Jy of flux. The third column, $S_{\rm min}$, lists the weakest source in the model, while the last column, $N$, lists the total number of sources. The case of 50% modeling corresponds to $f = 0.5$, and Table 4 shows that 50% of the total flux in the field will be contained in only two sources. This means that simple starting models for self-calibration (e.g., two point sources) should work well.

Table 4—Flux Density Available for Calibration at 74 MHz

| $f$ | $S_{\rm mod}$ (Jy) | $S_{\rm min}$ (Jy) | $N$ |
|---|---|---|---|
| 1.0 | 9.8 | 0.0036 | 167 |
| 0.75 | 7.3 | 0.12 | 10.2 |
| 0.50 | 4.9 | 0.91 | 2.0 |
| 0.25 | 2.5 | 4.0 | 0.25 |
| 0.10 | 1.0 | 14.2 | 0.04 |

Equations (1) and (2) can now be compared to show that for the LWA bank collecting areas described in Section 3.3 ($A_{\rm eff} \sim 10^3$ m$^2$ at 74 MHz), the confusion and thermal-noise contributions are comparable. From this approximation we calculate that the LWA described in Section 3.3 can achieve millijansky-level sensitivity in reasonable integration times, e.g., 0.5 to 1 mJy at 74 MHz for an 8-hour integration and 3-MHz bandwidth. Additional calculations presented in Section 3.3 (see Table 5) were made under this assumption.

### *3.2.3 Ionospheric Compensation*

The 74 and 330 MHz VLA systems demonstrate that self-calibration will successfully remove ionospheric phase effects when the full array signal-to-noise ratio is 3 to 5. Since the signal-to-noise ratio on an individual baseline is a factor of $N^{-1/2}$ times smaller than that available for an array of $N$ individual antennas (or banks of dipoles), an array of roughly 30 banks proposed in Section 3.3 would mean that we can tolerate a signal-to-noise ratio on a single baseline of approximately 1 and still have convergence. Perley and Erickson (1984) have calculated the signal-to-noise ratio available for self-calibration under the assumption that the noise is thermal noise from the Galactic background and that the FoV of the instrument will be comparable with or less than the isoplanatic patch size. For 50% modeling and 1° FoV, they find that a baseline-based signal-to-noise ratio of unity can be achieved by bank collecting areas of $A_{\rm eff} \sim 10^2$ m$^2$. Since the values of $A_{\rm eff}$ proposed in Section 3.3 (see also Table 5) are greater than this, a self-calibration–based approach to ionospheric compensation will work successfully for the proposed array. Experience with the present 74 MHz VLA system already confirms this expectation.

Dual-frequency ionospheric phase referencing (DFIPR), a technique for greatly increasing the robustness of self-calibration, has also been recently developed with the 74 MHz VLA. Ionospheric phase fluctuations are measured at 327 MHz and the corrections derived from 327 MHz are then be scaled to 74 MHz and used to "unwind" the effects of the ionosphere at this lower frequency (Kassim et al. 1993). Figure 17 illustrates this procedure. DFIPR significantly increases the coherence time of the data, thus allowing longer integration times for self-calibration. It has also been used to image 74 MHz VLA data without self-calibration. This could relax the LWA dependence on self-calibration, and therefore consideration should be made of designing an instrument with the capability of obtaining a concurrent higher frequency (greater than or equal to 100 MHz) data stream which could be used to track the ionospheric disturbances at the lower frequencies (less than or equal to 100 MHz).

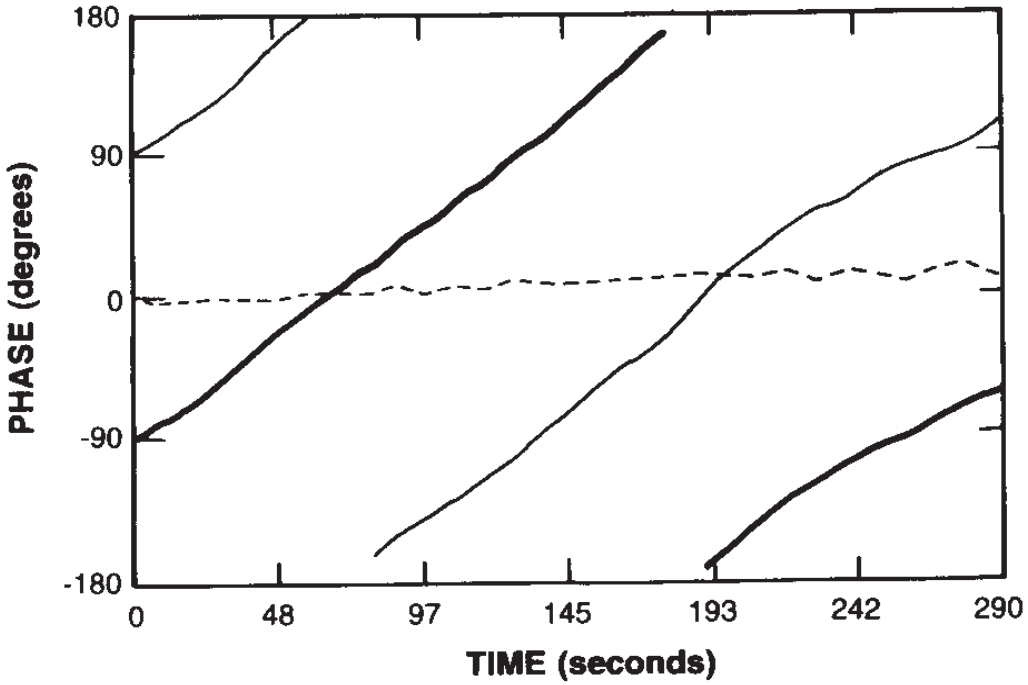


Fig. 17—Visibility phase *vs.* time on a 15-km baseline for a point source located at the phase center. The thick solid line is the phase measured at 74 MHz and the roughly 360° phase wind is from the ionosphere. The thin solid line is the ionospheric model derived from the simultaneous 330 MHz measurements. The dashed line represents the difference between the two. As can be seen, the "scaled" 330 MHz phases track the ionospheric phase variations quite well at 74 MHz.

### *3.2.4 Wide-Field Imaging*

A conventional two-dimensional inversion of the three-dimensional visibility function measured by non-coplanar (i.e., non–east-west) arrays introduces phase errors which can become severe at long wavelengths (Perley 1989). The phase error goes as $w\theta^2$, where $w$ is the third dimension in the visibility plane, perpendicular to the standard $u$-$v$ plane, and $\theta$ is the distance from the phase center. The "3-D problem" arises when the entire primary beam (i.e., $\theta$ large), which may contain hundreds of discrete sources at the wavelengths under consideration, must be properly deconvolved. Numerical solutions to this problem have now been successfully implemented within two widely used astronomical data reduction packages (SDE and AIPS), with their only limitation being the high computational expense. For example, SDE implements a polyhedron algorithm in which the 3-D "image volume" is split into many 2-D "facets," and is currently used to generate thermal-noise–limited images from 330 MHz VLA observations on a routine basis. Examples of successful wide-field, non-coplanar image deconvolutions are shown in Fig. 9 for the Galactic center at 330 MHz (from SDE) and Fig. 3 for the Coma cluster field at 74 MHz (from AIPS).

The computational driver for extending the polyhedron algorithm to longer wavelengths is the number of facets $N_{\rm facet}$ that are required to divide up the surface of the image sphere, and $N_{\rm facet} \propto \lambda B/D^2$, where $B$ is the baseline length, $\lambda$ is the observing wavelength, and $D$ is the aperture

size of the individual antenna elements (Perley 1989). For the 74 MHz VLA $N_{\rm facet} \sim 225$, so that for an instrument with $B$ greater than 100 km, thousands of facets may be required. Current scaled-processing platforms (e.g., SGI Origin 2000) have already demonstrated the capability of reducing data with hundreds of facets, and in light of the continuing rapid advance in available computational power, practical solutions to the wide-field imaging problem should be readily available for the LWA.

### *3.2.5 Radio Frequency Interference*

The LW spectrum contains copious amounts of radio frequency interference (RFI) from terrestrial transmitters. These interfering signals are, however, at low enough levels that they do not overload the highly linear electronics modules that are available on today's market at low prices. Experience has shown that sufficiently clear bands exist between the interfering signals to allow sensitive observations. In fact, the 74 MHz band at the VLA is one of the cleanest bands available to that instrument, and the radio band below 100 MHz is one of the few portions of the spectrum where RFI levels actually seem to be decreasing as many communication services move to higher frequencies or to optical fibers. Nevertheless, it will almost certainly be necessary to incorporate some RFI avoidance and excision procedures into the LWA system, but, with modern digital technology, this can be done relatively easily even for a correlator with many thousands of channels.

## 3.3 The LWA Concept

In this section we present an initial design for the LWA that can be used to estimate the various parameters involved in the construction of such a system. However, before any such instrument could be built, a detailed design study will be required. This design study may well result in significant changes to the proposal.

We envision crossed-dipole, log-periodic arrays, resembling large TV antennas, as the individual receiving elements. The elements will be pointed vertically and be mechanically fixed. The elements will be arranged into banks about 100-m square; each bank will contain $16 \times 16$ or 256 elements. The beam of a bank could be steered to any point in the sky by adjusting the phases of the individual elements within it. Beam steering would be entirely electronic, and no mechanical devices would be used. Figure 6 shows a possible LWA layout.

### *3.3.1 Frequency Range and Bandwidth*

The short-wavelength limit of the instrument is driven both by the scientific work that can be accomplished with the high–angular-resolution images that can be formed and by the necessity of self-calibrating these images. The phase information obtained from self-calibration is required for calibration of all longer-wavelength images using DFIPR (Kassim et al. 1993; see also Section 3.2.3). However, the effective collecting area of the system is proportional to $\nu^{-2}$, and at too high a frequency the antennas do not collect sufficient signal power for self-calibration. Based on these considerations, the nominal short-wavelength limit is 2 m (150 MHz) for the instrument, though an innovative plan to use active dipole elements might expand the upper end of the frequency range to 1 m (300 MHz).

The LW limit determines the physical size of the individual antenna elements. Assuming that dipoles are used in the log-periodic elements, the dipoles must be approximately one-half wavelength long at the LW limit. A major portion of the cost of the system is in the antenna elements; larger elements are much more costly. Also, the antenna elements must be separated by more than a half wavelength at the LW limit, and this rather large separation leads to troublesome grating responses at the shorter wavelengths. Another consideration at LWs is ionospheric amplitude scintillations. The phase variations scale precisely as $\lambda$ provided that no amplitude scintillations are present, and this precise scaling is used for calibration of the LW data (via DFIPR). However, at LWs there is enough angular refraction in ionospheric irregularities that rays passing through different irregularities can cross, causing constructive and destructive interference. This causes the apparent amplitude of the signal to scintillate and its phase to wander in an almost random fashion, making phase calibration virtually impossible. At most mid-latitude sites, amplitude scintillation will occur about 30% of the time at frequencies below 30 MHz, making the data unusable for this fraction of the time. Thus, some operation with diminished efficiency down to around 15 MHz should be possible under particularly quiet ionospheric conditions.

Thus, we propose an instrument that is designed to operate in the frequency range of 15 to 150 MHz, but with somewhat less efficiency in the 15 to 30 MHz range. Table 5 lists approximate LWA specifications.

Table 5—LWA Specifications

| | |
|---|---|
| Frequency range | 15–150 MHz |
| Bandwidth | 0.05–3.0 MHz |
| Total collecting area | $10^6$ m$^2$ @ 15 MHz |
| | $10^4$ m$^2$ @ 150 MHz |
| Angular resolution | $8''$ @ 15 MHz |
| | $0\farcs8$ @ 150 MHz |
| Pointing/frequency conversion time | $< 1$ ms |
| Sky coverage | $< 60^\circ$ zenith distance |
| Sensitivity ($\Delta\nu = 3$ MHz, $t = 8$ hr) | $\sim 1$ mJy @ 15 MHz |
| | $\sim 0.3$ mJy @ 150 MHz |
| Polarization | Full |
| Field of view | $\sim 6^\circ$ @ 15 MHz |
| | $\sim 0\fdg7$ @ 150 MHz |
| Number of instantaneous baselines | 435 |
| Time resolution | 10 ms |

### *3.3.2 The Array Configuration*

The log-periodic elements will be arranged into banks; each bank is the analog of a single antenna in a system like the VLA. The banks would probably be square or rectangular in shape, and each bank must provide enough collecting area for self-calibration at 150 MHz. This requires about 256 elements per bank, which will provide about 350 m$^2$ at 150 MHz; at 15 MHz, the collecting area of each bank will be 35 000 m$^2$.

We propose that a total of 30 banks be constructed in two stages. A first stage would be the construction of 15 banks in an area some 30 km in diameter. This would comprise a "compact" array that would have angular resolutions of $2'$ at 15 MHz and $12''$ at 150 MHz. It would be sensitive to extended structures and would be particularly useful for the study of extended Galactic objects (e.g., SNRs) and as a solar radar receiver. Data transfer between the banks and a central laboratory would be by optical fibers.

A second stage would be the construction of another 15 banks in a Y-shaped configuration some 500 km in diameter. When combined with the compact array, this "extended" array would have angular resolutions of $8''$ at 15 MHz and $0\farcs8$ at 150 MHz. Data transfer via optical fibers over the distances required would be expensive; a more practical solution may be to record the data at each bank or to transfer the data via microwave links. If the central array is sited at the VLA, the extended array could evolve with the VLA Expansion Project whose "A+ configuration" would provide the arc-second angular resolution desired for many LWA extragalactic source studies.

### *3.3.3 The Array Site*

We consider the NRAO VLA site in New Mexico to be an advantageous site for the LWA, assuming that appropriate arrangements could be made with the NRAO. The land could probably be made available fairly easily and the size of the VLA site matches the requirements for the compact portion of the LWA. A strong infrastructure for radio astronomy already exists at the site, and unused buildings exist that might be used for a central laboratory. There is a proposal for extensions to the present VLA that would involve new antennas in a region roughly 500 km in diameter surrounding the present VLA. The sites for these dishes would be appropriate for the extended banks of the LWA. These extended sites will be equipped for optical fiber communication with the central site.

Other good sites do exist, but the VLA site would be the most convenient and least expensive LWA location. We anticipate developing a central array around the present VLA site, and then based on experience, expanding the geometry along with the VLA upgrade. Moreover, bistatic Arecibo-LWA imaging solar radar observations would be possible for a period of up to 2.6 hr centered on Arecibo local noon for a southwestern U.S. LWA location, and the current VLA site is more than large enough for the requirements of the solar radar receiving array.

### *3.3.4 Cost*

A detailed cost analysis for the LWA has not yet been prepared, but Table 6 contains order-of-magnitude estimates. The main point is that the cost of such an array would be measured in the millions of dollars, as opposed to the hundreds of millions required for higher-frequency ground- or space-based systems of comparable size or sophistication. The main savings are realized because of the cheap cost of the wire antenna elements and the simple, uncooled electronics that are required to process the radio signals of modest bandwidth in this frequency regime.

Table 6—Order-of-Magnitude LWA Costs

| Item | Estimated cost (USD) |
|---|---|
| Antenna Element | |
| pole | 10 |
| wire and insulators | 10 |
| balun and preamp | 10 |
| coaxial cable (40 m) | 40 |
| Total | 70 |
| Antenna Bank | |
| 256 antenna elements | 18k |
| phasing network | 60k |
| Control system | 100k |
| Data transmission (fiber-optic link) | 160k |
| Total | 338k |
| Array | |
| 30 banks | 10M |
| labor and travel | 10M |
| data processing facility | 5M |
| **Total** | 25M |

## 4. SUMMARY

### 4.1 Technical Summary

The proposed LWA will open a new, high-resolution window on the electromagnetic spectrum from 15 to 150 MHz (corresponding to wavelengths of 2 to 20 m). This region has been poorly explored because ionospheric structure prevents conventional interferometry on baselines longer than 5 km, limiting imaging to coarse angular resolution and sensitivity. Development of ionospheric phase-compensation techniques on the NRL-NRAO 74 MHz VLA receiving system now make it possible to explore this region at unprecedented angular resolution.

The LWA will be a powerful instrument for delineating the interaction between nonthermal emitting plasmas and thermal absorbing gas, for differentiating between self-absorption processes, and for exploring the universe for coherent emission processes. For solar, planetary, Galactic, and extragalactic work it will provide unique information on the distributions of ionized gas, relativistic particles, and magnetic fields. The distribution and spectrum of the cosmic-ray electron gas, high-redshift radio galaxies and quasars, shocks driven by infalling matter in clusters of galaxies, pulsars in the Milky Way and in external galaxies, and radio emission from extrasolar planets are all steep-spectrum processes that could be especially well studied. It is also the ideal receiver for proposed solar radar systems that can be used to image Earthward-bound CMEs for geomagnetic storm prediction.

We propose a long wavelength array to conduct these observations. The LWA will be a large (greater than 100 km), electronic, broadband instrument providing fast (less than 1 ms) frequency selection and pointing, capable of imaging radio sources across the sky and spectrum rapidly. By using wire antennas and low-cost, readily available electronic components, we can construct the LWA at a significantly lower cost than that for higher frequency ground or space-based systems of comparable size or sophistication.

### 4.2 Potential LWA Consortia

Groups at NRL and NFRA are interested in developing the LWA. These joint interests have spurred initial discussions to develop a consortium, and could be expanded to include university or other partners. Synergetic coordination of the LWA with planned expansions of existing higher-frequency facilities could enable mutual sharing of infrastructure and development costs.

An NRL- and NFRA-led consortium provides an excellent strategic opportunity to realize the LWA within the next decade. With no significant technology hurdles to overcome, an LWA situated in the southwestern U.S., for example, would be ideally suited for carrying out both basic astrophysics investigations as well as bistatic solar radar studies with Arecibo. In this case the LWA would achieve natural synergy with both SKA development plans and the VLA upgrade.

## 5. ACKNOWLEDGMENTS

We thank D. Backer, T. Bastian, K. Blundell, P. Crane, J. Cordes, N. Duric, T. Ensslin, W. Farrell, P. Ray, L. J Rickard, R. Stubner, and A. Vourlidas for helpful comments. The National Radio Astronomy Observatory is a facility of the National Science Foundation operated under

cooperative agreement by Associated Universities, Inc. Basic research in radio astronomy at the Naval Research Laboratory is supported by the Office of Naval Research.

## 6. REFERENCES

Alexander, P. and J.P. Leahy (1987). "Aging and Speeds in a Representative Sample of 21 Classical Double Radio Sources," *Mon. Not. R. Astron. Soc.* **225**, 1–26.

Anderson, M.C. and L. Rudnick (1996). "Sites of Relativistic Particle Acceleration in Supernova Remnant Cassiopeia A," *Astrophys. J.* **456**, 234–249.

Bell, A.R. (1978a). "The Acceleration of Cosmic Rays in Shock Fronts. I," *Mon. Not. R. Astron. Soc.* **182**, 147–156.

Bell, A.R. (1978b). "The Acceleration of Cosmic Rays in Shock Fronts. II," *Mon. Not. R. Astron. Soc.* **182**, 443–455.

Bietenholz, M.F., N. Kassim, D.A. Frail, R.A. Perley, W.C. Erickson, and A.R. Hajian (1997). "The Radio Spectral Index of the Crab Nebula," *Astrophys. J.* **490**, 291–301.

Blandford, R.D. and M.J. Rees (1974). "A 'Twin-Exhaust' Model for Double Radio Sources," *Mon. Not. R. Astron. Soc.* **165**, 395–415.

Blundell, K.M., S. Rawlings, and C.J. Willott (1999). "The Nature and Evolution of Classical Double Radio Sources from Complete Samples," *Astron. J.* **117**, 677–706.

Blundell, K.M., S. Rawlings, S.A. Eales, G.B. Taylor, and A.D. Bradley (1998). "A Sample of 6C Radio Sources Designed to Find Objects at Redshift $z > 4$—I. The Radio Data," *Mon. Not. R. Astron. Soc.* **295**, 265–279.

Bowyer, S. and T.W. Berghöfer (1998). "Inverse Compton Scattering as the Source of Diffuse Extreme-Ultraviolet Emission in the Coma Cluster of Galaxies," *Astrophys. J.* **506**, 502–508.

Bowyer, S., R. Lieu, and J.P. Mittaz (1998). "Diffuse EUV Emission from Clusters of Galaxies," in *IAU Symposium 188: The Hot Universe*, eds. K. Koyama, S. Kitamoto, and M. Itoh (Dordrecht: Kluwer) p. 185–188.

Bowyer, S., M. Lampton, and R. Lieu (1996). "Extreme-Ultraviolet Flux from the Virgo Cluster: Further Evidence for a 500,000-Kelvin Component," *Science* **274**, 1338–1340.

Beuermann, K., G.O. Kanbach, and E.M. Berkhuijsen (1985). "Radio Structure of the Galaxy—Thick Disk and Thin Disk at 408 MHz," *Astron. & Astrophys.* **153**, 17–34.

Carilli, C.L., R.A. Perley, J.W. Dreher, and J.P. Leahy (1991). "Multifrequency Radio Observations of Cygnus A. Spectral Aging in Powerful Radio Galaxies," *Astrophys. J.* **383**, 554–573.

Carr, T.D. and L. Wang (1990). "Monitoring Jupiter's Hectometric Emission," in *Low Frequency Astrophysics from Space*, eds. N.E. Kassim and K.W. Weiler (Heidelberg: Springer-Verlag) p. 113–117.

Cordes, J.M. (1990). "Low Frequency Interstellar Scattering and Pulsar Observations," in *Low Frequency Astrophysics from Space*, eds. N.E. Kassim and K.W. Weiler (Berlin: Springer-Verlag) p. 165–174.

Cordes, J.M. and B.J. Rickett (1998). "Diffractive Interstellar Scintillation Timescales and Velocities," *Astrophys. J.* **507**, 846–860.

Cordes, J.M. and T.J.W. Lazio (1997). "Finding Radio Pulsars in and beyond the Galactic Center," *Astrophys. J.* **475**, 557–564.

De Breuck, C., M.S. Brotherton, H.D. Tran, W. van Breugel, and H.J.A. Röttgering (1998). "Discovery of an Ultra-Steep-Spectrum, Highly Polarized Red Quasar at $z = 1.462$," *Astron. J.* **116**, 13–19.

de Pater, I. (1999). private communication

DeForest, C. (1996). "Lock-In Detection of Network-Driven Waves in the Corona," SOHO Joint Observing Program, 52.

Dewey, R.J., J.H. Taylor, J.M. Weisberg, and G.H. Stokes (1985). "A Search for Low-Luminosity Pulsars," *Astrophys. J.* **294**, L25–L29.

Donnelly, R.H., M. Markevitch, W. Forman, C. Jones, L.P. David, E. Churazov, and M. Gilfanov (1998). "Temperature Structure in Abell 1367," *Astrophys. J.* **500**, 138–146.

Dulk, G.A., Y. Leblanc, and T.S. Bastian (1997). "Search for Cyclotron-maser Radio Emission from Extrasolar Planets," *BAAS* DPS meeting **29**, 28.03.

Dulk, G.A. and O.B. Slee (1975). "Spectral Turnovers of Galactic Supernova Remnants," *Astrophys. J.* **199**, 61–68.

Duric, N., S.M. Gordon, W.M. Goss, F. Viallefond, and C. Lacey (1995). "The Relativisitic ISM in M33: Role of the Supernova Remnants," *Astrophys. J.* **445**, 173–181.

Duric, N., F. Viallefond, W.M. Goss, and J.M. van der Hulst (1993). "The VLA-WSRT Survey of M33—Statistical Properties of a Sample of Optically Selected Supernova Remnants," *Astron. & Astrophys. Suppl.* **99**, 217–255.

Ellison, D.C., S.P. Reynolds, K. Borkowski, R. Chevalier, D.P. Cox, J.R. Dickel, R. Pisarski, J. Raymond, S.R. Spangler, H.J. Volk, and J.P. Wefel (1994). "Supernova Remnants and the Physics of Strong Shocks," *Pub. Astron. Soc. Pacific* **701**, 780–797.

Ensslin, T.A., R. Lieu, and P.L. Biermann (1999). "Non-thermal Origin of the EUV and HEX Excess Emission of the Coma Cluster—The Nature of the Energetic Electrons," *Astron. & Astrophys.* **344**, 409–420.

Ensslin, T.A. and P.L. Biermann (1998). "Limits on Magnetic Fields and Relativistic Electrons in the Coma Cluster from Multifrequency Observations," *Astron. & Astrophys.* **330**, 90–96.

Ensslin, T.A., P.L. Biermann, U. Klein, and S. Kohle (1998a). "Cluster Radio Relics as a Tracer of Shock Waves of the Large-Scale Structure Formation," *Astron. & Astrophys.* **332**, 395–409.

Ensslin, T.A., Y. Wang, B.B. Nath, and P.L. Biermann (1998b). "Black Hole Energy Release to the Gaseous Universe," *Astron. & Astrophys.* **333**, L47–L50.

Erickson, W.C., D. McConnell, and K.R. Anantharamaiah (1995). "Low-Frequency Carbon Recombination Lines in the Central Regions of Galaxy," *Astrophys. J.* **454**, 125–133.

Erickson, W.C. and M.J. Mahoney (1985). "The Radio Continuum Spectrum of PSR 1937+214," *Astrophys. J.* **299**, L29–L31.

Erickson, W.C., M.J. Mahoney, and K. Erb (1982). "The Clark Lake Teepee-Tee telescope," *Astrophys. J. Suppl.* **50**, p. 403–419.

Fanaroff, B.L. and J.M. Riley (1974). "The Morphology of Extragalactic Radio Sources of High and Low Luminosity," *Mon. Not. R. Astron. Soc.* **167**, 31P–36P.

Farrell, W.M., M.D. Desch, and P. Zarka (1999). "On the Possibility of Coherent Cyclotron Emission from Extrasolar Planets," *J. Geophys. Res. (Planets)* **104**, 14025–14032.

Frail, D.A., P.J. Diamond, J.M. Cordes, and H.J. van Langevelde (1994). "Anisotropic Scattering of OH/IR Stars toward the Galactic Center," *Astrophys. J.* **427**, L43–L46.

Gil J.A., D.G. Khechinashvili, and G.I. Melikidze (1998). "On the Radio-Frequency Emission from the Geminga Pulsar," *Mon. Not. R. Astron. Soc.* **298**, 1207–1211.

Gnedin, N.Y. and J.P. Ostriker (1997). "Reionization of the Universe and the Early Production of Metals," *Astrophys. J.* **486**, 581–598.

Gordon, S.M., R.P. Kirshner, K.S. Long, W.P. Blair, N. Duric, and R.C. Smith (1998). "A New Optical Sample of Supernova Remnants in M33," *Astrophys. J. Suppl.* **117**, 89–133.

Gordon, I.M. (1968). "Interpretation of Radio Echos from the Sun," *Astrophys. Lett.* **2**, 49–53.

Gosling, J.T., E. Hildner, R.M. MacQueen, R.H. Munro, A.I. Poland, and C.L. Ross (1974). "Mass Ejections from the Sun: A View from Skylab," *J. Geophys. Res.* **79**, 4581–4587.

Green, D.A. (1991). "Limitations Imposed on Statistical Studies of Galactic Supernova Remnants by Observational Selection Effects," *Pub. Astron. Soc. Pacific* **103**, 209–220.

Gwinn, C.R., N. Bartel, and J.M. Cordes (1993). "Angular Broadening of Pulsars and the Distribution of Interstellar Plasma Fluctuations," *Astrophys. J.* **410**, 673–685.

Hales, S.E.G., J.E. Baldwin, and P.J. Warner (1993). "The 6C Survey of Radio Sources. VI. The Continuous Zone $\delta$ between 30° and 51°, $\alpha$ between $00^{\rm h}$ and $09^{\rm h}$ $05^{\rm m}$ and $\alpha$ between $22^{\rm h}$ $35^{\rm m}$ and $24^{\rm h}$," *Mon. Not. R. Astron. Soc.* **263**, 25–30.

Hamilton, A.J.S. and R.A. Fesen (1988). "The Reionization of Unshocked Ejecta in SN 1006," *Astron. J.* **327**, 178–196.

Haslam, C.G.T., C.J. Salter, H. Stoffel, and W.E. Wilson (1981). "A 408 MHz All-Sky Continuum Survey. II–The Atlas of Contour Maps," *Astron. & Astrophys. Suppl.* **47**, 1–142.

Heeschen D.S. (1960). "A Color-Absolute Magnitude Diagram for Extragalactic Radio Sources," *Pub. Astron. Soc. Pacific* **72**, 368–376.

Hess, V. (1912). "Über Beobachtungen der durchdringenden Strahlung bei sieben Freiballonfahrten," *Phys. Z.* **13**, 1084–1091.

Hewish, A., S.J. Bell, J.D.H. Pilkington, P.F. Scott, and R.A. Collins (1968). "Observation of a Rapidly Pulsating Radio Source," *Nature* **217**, 709–713.

Hummel, E. (1991). "On the Low Frequency Radio Spectrum of Spiral Galaxies," *Astron. & Astrophys.* **251**, 442–446.

Hwang C.-Y. (1997). "An Inverse Compton Process for the Excess Diffuse EUV Emission from Virgo and Coma Galaxy Clusters," *Science* **278**, 1917–1919.

Ishimaru, A. and R. Woo (1978). "Interpretation of Radar Measurements of the Sun," $E \oplus S$ **59**, 1175.

Israel, F.P., M.J. Mahoney, and N. Howarth (1992). "The Integrated Radio Continuum Spectrum of M33—Evidence for Free-Free Absorption by Cool Ionized Gas," *Astron. & Astrophys.* **261**, 47–56.

Israel, F.P. and M.J. Mahoney (1990). "Low-Frequency Radio Continuum Evidence for Cool Ionized Gas in Normal Spiral Galaxies," *Astrophys. J.* **352**, 30–43.

James, J.C. (1968). "Radar Studies of the Sun," in *Radar Astronomy*, eds. J.V. Evans and T. Hagfors (New York: McGraw-Hill) p. 323–385.

James, J.C. (1970). "Some Observed Characteristics of Solar Radar Echoes and Their Implications," *Solar Phys.* **12**, 143–162.

Jansky, K.G. (1933). "Electrical Disturbances Apparently of Extraterrestrial Origin," *Proc. I. R. E.* **21**, 1387–1398.

Jones, T.W., et al. (1998). "$10^{51}$ Ergs: The Evolution of Shell Supernova Remnants," *Publ. Astron. Soc. Pacific* **110**, 125–151.

Kassim, N.E. and T.J.W. Lazio (1999). "Upper Limits on the Continuum Emission from the Geminga Pulsar at 74 and 327 MHz," *Astrophys. J.* **527**, L101–L104.

Kassim, N.E. and W.C. Erickson (1998). "Meter/Decameter Wavelength Array for Astrophysics and Solar Radar," in *Advanced Technology MMW, Radio, and Terahertz Telescopes*, SPIE **3357**, 740–754.

Kassim, N.E., T.N. LaRosa, T.J.W. Lazio, and S. Hyman (1999). "Wide-Field Radio Imaging of the Galactic Center," in *The Central Parsecs*, eds. H. Falke, A. Cotera, W.J. Duschl, F. Melia, and M.J. Rieke (San Francisco: ASP) p. 403–414.

Kassim, N.E. and D.A. Frail (1996). "A New Supernova Remnant over the Galactic Centre," *Mon. Not. R. Astron. Soc.* **283**, L51–L57.

Kassim, N.E., R.A. Perley, C.L. Carilli, D.E. Harris, and W.C. Erickson (1995a). "Low Frequency Observations of Cygnus A," in *Cygnus A: Study of a Radio Galaxy*, eds. C.L. Carilli and D.E. Harris, (Cambridge: Cambridge University Press) p. 182–190.

Kassim, N.E., R.A. Perley, K.S. Dwarakanath, and W.C. Erickson (1995b). "Evidence for Thermal Absorption inside Cassiopeia A," *Astrophys. J.* **455**, L59–L62.

Kassim, N.E., R.A. Perley, W.C. Erickson, and K.S. Dwarakanath (1993). "Subarcminute Resolution Imaging of Radio Sources at 74 MHz with the Very Large Array," *Astron. J.* **106**, 2218–2228.

Kassim, N.E. (1990)."H II Regions in Absorption at Low Frequencies," in *Low Frequency Astrophysics from Space*, eds. N.E. Kassim and K.W. Weiler (Heidelberg: Springer-Verlag) p. 144–151.

Kassim, N.E. (1989). "Low Frequency Observations of Galactic Supernova Remnants and the Distribution of Low Density Gas in the Interstellar Medium," *Astrophys. J.* **347**, 915–924.

Kassim, N.E., K.W. Weiler, W.C. Erickson, and T.C. Wilson (1989). "Improved Estimates of Galactic H II Region Emission Measures and Filling Factors: Low-Frequency VLA Observations near Sharpless 53", *Astrophys. J.* **338**, 152–161.

Kronberg, P.P. (1999). private communication

Kronberg, P.P. (1990). "Radio Emission from Intergalactic Gas and Its Implications for Low Frequency Astronomy in Space," in *Low Frequency Astrophysics from Space*, eds. N.E. Kassim and K.W. Weiler (Heidelberg: Springer-Verlag) p. 262–268.

Kundu, M.R. (1965). "Radar Observations of the Sun," in *Solar Radio Astronomy* (New York: Wiley) Ch. 17, p. 627–632.

Kuz'min, A.D. and B.Ya. Losovskii (1997). "PSR J0633+1746," *IAU Circ.*, 6559.

Kuz'min, A.D. and B.Ya. Losovskii (1997). "Detection of the Radio Pulsar PSR J0633+1746 in Geminga," *Pis'ma Astron. Zh.* **23**, 323–325 (transl. *Astron. Lett.* **23**, 283).

Lacey, C.K. (1998). Ph.D. Thesis, University of New Mexico.

Laing, R.A. and J.A. Peacock (1980). "The Relation between Radio Luminosity and Spectrum for Extended Extragalactic Radio Sources," *Mon. Not. R. Astron. Soc.* **190**, 903–924.

Lazio, T.J.W. and J.M. Cordes (2001). "A VLA Survey for Radio Pulsars in and Beyond the Galactic Center," *Astrophys. J. Suppl.*, in preparation.

Lazio, T.J.W. and J.M. Cordes (1998). "Hyperstrong Radio-Wave Scattering in the Galactic Center. II. A Likelihood Analysis of Free Electrons in the Galactic Center," *Astrophys. J.* **505**, 715–731.

Lemoine, M., G. Sigl, A.V. Olinto, and D.N. Schramm, (1997). "Ultra–high-Energy Cosmic-Ray Sources and Large-Scale Magnetic Fields," *Astrophys. J.* **486**, L115–L118.

Lerche, I. and R. Schlickeiser (1982a). "On the Transport and Propagation of Cosmic Rays in Galaxies. I. Solution of the Steady-State Transport Equation for Cosmic Ray Nucleons, Momentum Spectra and Heating of the Interstellar Medium," *Mon. Not. R. Astron. Soc.* **201**, 1041–1072.

Lerche, I. and R. Schlickeiser (1982b). "Transport and Propagation of Cosmic Rays in Galaxies. II. The Effect of a Galactic Wind on the Mean Lifetime and Age Distribution of Non-Decaying Cosmic Rays," *Astron. & Astrophys.* **116**, 10–26.

Lieu, R., et al. (1996). "Diffuse Extreme-Ultraviolet Emission from the Coma Cluster: Evidence for Rapidly Cooling Gases at Submegakelvin Temperatures," *Science* **274**, 1335–1338.

Longair, M.S. (1990). "Cosmic Rays and the Galactic Radio Background Emission," in *Low Frequency Astrophysics from Space*, eds. N.E. Kassim and K.W. Weiler (Heidelberg: Springer-Verlag) p. 227–236.

Lozinskya, T.A. (1992). *Supernovae and Stellar Wind in the Interstellar Medium* (New York: AIP).

Lyne, A.G., et al. (1998). "The Parkes Southern Pulsar Survey—II. Final Results and Population Analysis," *Mon. Not. R. Astron. Soc.* **295**, 743–755.

Mahoney, M.J. and W.C. Erickson (1985). "A Fast Pulsar Candidate in the Globular Cluster M28," *Nature* **317**, 154–155.

Maia, D., A. Vourlidas, M. Pick, R.A. Howard, R. Schwenn, and A. Magalhães (1999). "Radio Signatures of a Fast Coronal Mass Ejection Development," *J. Geophys. Res.*(Space Physics) **104**, 12507–12514.

Malofeev, V.M. and O.I. Malov (1997). "Detection of Geminga as a Radio Pulsar," *Nature* **389**, 697–699.

Malov, I.F. (1998). "Why Does Geminga Have Such a Low Radio Luminosity?" *Astron. Rep.* **42**, 246–251.

Manchester, R.N., et al. (1996). "The Parkes Southern Pulsar Survey–I. Observing and Data Analysis Systems and Initial Results," *Mon. Not. R. Astron. Soc.* **279**, 1235–1250.

Markevitch, M., W.R. Forman, C.L. Sarazin, and A. Vikhlinin (1998). "The Temperature Structure of 30 Nearby Clusters Observed with ASCA: Similarity of Temperature Profiles," *Astrophys. J.* **503**, 77–96.

Markevitch, M., C.L. Sarazin, and A. Vikhlinin (1999). "Physics of the Merging Clusters Cygnus A, A3667, and A2065," *Astrophys. J.* **521**, 526–530.

Mittaz, J.P.D., R. Lieu, and F.J. Lockman (1998). "Detection of Luminous Intracluster Extreme-Ultraviolet Emission From Abell 1795," *Astrophys. J.* **498**, L17–L20.

Moran, J.M., L.F. Rodríguez, B. Greene, and D.C. Backer (1990). "The Large Scattering Disk of NGC 6334B," *Astrophys. J.* **348**, 147–152.

Myers, S.T. and S.R. Spangler (1985). "Synchrotron Aging in the Lobes of Luminous Radio Galaxies," *Astrophys. J.* **291**, 52–62.

Navarro, J, A.G. de Bruyn, D.A. Frail, S.R. Kulkarni, and A.G. Lyne (1995). "A Very Luminous Binary Millisecond Pulsar," *Astrophys. J.* **455**, L55–58.

Owen, F.N., J.A. Eilek, and N.E. Kassim (2000). "M 87 at 90 Centimeters: A Different Picture," *Astrophys. J.* **543**, 611–619.

Parrish, A. (1968). "Solar Radar Experiments, 1967," Technical Report 300, Center for Radiophysics and Space Research, Cornell University, Ithaca, New York

Payne, H.E., K.R. Anantharamaiah, and W.C. Erickson (1994). "High Rydberg State Carbon Recombination Lines Towards Cas A: Physical Conditions and a New Class of Models," *Astrophys. J.* **430**, 690–705.

Pedlar, A., K.R. Anantharamaiah, R.D. Ekers, W.M. Goss, and J.H. van Gorkom (1989)."Radio Studies of the Galactic Center. I. The Sagittarius A Complex," *Astrophys. J.* **342**, 769–784.

Perley, R.A. and W.C. Erickson (1984). "A Proposal for a Large, Low Frequency Array Located at the VLA Site," VLA Scientific Memorandum 146. (Socorro: National Radio Astronomy Observatory).

Perley, R.A. (1989). "Imaging with Non-coplanar Arrays," in *Synthesis Imaging in Radio Astronomy*, eds. R.A. Perley, F.R. Schwab, and A.H. Bridle (San Francisco: ASP) p. 259–275.

Ramachandran, R., A.A. Deshpande, and C. Indrani (1998). "Upper Limits on the Pulsed Radio Emission from the Geminga Pulsar at 35 and 327 MHz," *Astron. & Astrophys.* **339**, 787–790.

Rawlings, S., M. Lacy, K.M. Blundell, S.A. Eales, A.J. Bunker, and S.T. Garrington (1996). "A Radio Galaxy at Redshift 4.41," *Nature* **383**, 502–505.

Reber, G. (1940). "Cosmic Static," *Astrophys. J.* **91**, 621–624.

Reynolds, S.P. and D.C. Ellison (1992). "Electron Acceleration in Tycho's and Kepler's Supernova Remnants. Spectral Evidence of Fermi Shock Acceleration," *Astrophys. J.* **399**, L75–L78.

Rodriguez, P. (1996). "High Frequency Radar Detection of Coronal Mass Ejections," in *Solar Drivers of Interplanetary and Terrestrial Disturbances*, eds. K.S. Balasubramaniam, S.L. Keil, and R.N. Smartt (San Francisco: Astronomical Society of the Pacific) p. 180–188.

Roettiger, K., J.O. Burns, and J. Pinkney (1995). "On the Origin of Temperature Substructure within Merging Clusters of Galaxies: Abell 2256," *Astrophys. J.* **453**, 634–640.

Röttgering, H.J.A., M.H. Wieringa, R.W. Hunstead, and R.D. Ekers (1997). "The Extended Radio Emission in the Luminous X-ray Cluster A3667," *Mon. Not. R. Astron. Soc.* **290**, 577–584.

Rudnick, L., D.M. Katz-Stone, and M.C. Anderson (1994). "Do Relativistic Electrons Either Gain or Lose Energy Outside of Extragalactic Nuclei?," *Astrophys. J. Suppl.* **90**, 955–958.

Sarazin, C.L. (1999). "The Energy Spectrum of Primary Cosmic Ray Electrons in Clusters of Galaxies and Inverse Compton Emission", *Astrophys. J.* **520**, 529–547.

Sarazin, C.L. and R. Lieu (1998). "Extreme-Ultraviolet Emission from Clusters of Galaxies: Inverse Compton Radiation from a Relic Population of Cosmic Ray Electrons?" *Astrophys. J.* **494**, L177–L180.

Schaefer, B.E., J.R. King, C.P. Deliyannis, and E.P. Rubenstein (1999). "Superflares on Normal F8–G8 Main Sequence Stars," *BAAS* **193**, 22.01.

Scheuer, P.A.G. (1974). "Models of Extragalactic Radio Sources with Continuous Energy Supply from a Central Object," *Mon. Not. R. Astron. Soc.* **166**, 513–528.

Schlickeiser, R., A. Sievers, and H. Thiemann (1987). "The Diffuse Radio Emission from the Coma Cluster," *Astron. & Astrophys.* **182**, 21–78.

Shaver, P.A., R.A. Windhorst, P. Madau, and A.G. de Bruyn (1999). "Can the Reionization Epoch Be Detected as a Global Signature in the Cosmic Background?" *Astron. & Astrophys.* **345**, 380–390.

Shitov, Yu.P., V.M. Malofeev, O.I. Malov, and V.D. Pugachev (1997). "PSR J0633+1746," *IAU Circ.*, 6775.

Shitov, Yu.P. and V.D. Pugachev (1997). "The Radio Pulsar Geminga," *New Astron.* **3**, 101–109.

Shrauner, J.A., J.H. Taylor, and G. Woan (1998). "The Second Cambridge Pulsar Survey at 81.5 MHz," *Astrophys. J.* **509**, 785–792.

Sigl, G. and M. Lemoine (1998). "Reconstruction of Source and Cosmic Magnetic Field Characteristics from Clusters of Ultra-High Energy Cosmic Rays," *Astroparticle Phys.* **9**, 65–78.

Spangler, S.R. and J.M. Cordes (1998). "VLBI Measurements of Plasma Turbulence Associated with the Cygnus OB1 Association," *Astrophys. J.* **505**, 766–783.

Spangler, S.R., R.L. Mutel, J.M. Benson, and J.M. Cordes (1986). "Interstellar Scattering of Compact Radio Sources near Supernova Remnants," *Astrophys. J.* **301**, 312–319.

Strong, A.W., et al. (1996). "Diffuse Galactic Hard X-Ray and Low-Energy Gamma-Ray Continuum," *Astron. & Astrophys. Suppl.* **120**, 381–387.

Subrahmanyan, R. and W.M. Goss (1996). "Electorn Temperatures in the Galactic H II Regions W43 and M17," *Mon. Not. R. Astron. Soc.* **281**, 239–244.

Tauris, T.M., et al. (1994). "Discovery of PSR J0108−1431: The Closest Known Neutron Star?" *Astrophys. J.* **428**, L53–L55.

Taylor, J.H. and J.M. Cordes (1993). "Pulsar Distances and the Galactic Distribution of Free Electrons," *Astrophys. J.* **411**, 674–684.

Tozzi, P., P. Madau, A. Meiksin, and M.J. Rees (1999). "Radio Signatures of H I at High Redshift: Mapping the End of the 'Dark Ages'," *Astrophys. J.* **528**, 597–606.

Vats, H.O., M.R. Deshpande, C. Shah, A.K. Singal, K.N. Iyer, R. Oza, and S. Doshi (1997). "Geminga," *IAU Circ.*, 6699.

Wardle, J.F.C., D.C. Homan, R. Ojha, and D.H. Roberts (1998). "Electron-Positron Jets Associated with the Quasar 3C 279," *Nature* **395**, 457–461.

Walker, M.A. (1998). "Interstellar Scintillation of Compact Extragalactic Radio Sources," *Mon. Not. R. Astron. Soc.* **294**, 307–311.

Webber, W.R. (1990). "Cosmic Rays in the Galaxy and Their Implications for Very Low Frequency Radio Astronomy," in *Low Frequency Astrophysics from Space*, eds. N.E. Kassim and K.W. Weiler (Heidelberg: Springer-Verlag) p. 217–226.

Weiler, K.W. (1990). "Low Frequency Astrophysics with a Space Array," in *Low Frequency Astrophysics from Space*, eds. N.E. Kassim and K.W. Weiler (Heidelberg: Springer-Verlag) p. 8–18.

Wentzel, D.G. (1981). "A New Interpretation of James' Solar Radar Echoes Involving Lower-Hybrid Waves," *Astrophys. J.* **248**, 1132–1143.

Werner, W. (1988). "Detection of the Galactic Wind Effect for the Cosmic Ray Propagation in the Edge-on Galaxy NGC 4631," *Astron. & Astrophys.* **201**, 1–8.

Wills, K.A., A. Pedlar, T.W.B. Muxlow, and P.N. Wilkinson (1997). "Low-Frequency Observations of Supernova Remnants in M82," *Mon. Not. R. Astron. Soc.* **291**, 517–526.

Yusef-Zadeh, F., W. Cotton, M. Wardle, F. Melia, and D.A. Roberts (1994). "Anisotropy in the Angular Broadening of Sagittarius A* at the Galactic Center," *Astrophys. J.* **434**, L63–L66.

Zhao, J.-H., et al. (1992). "A Transient Radio Source near the Center of the Milky Way Galaxy," *Science* **255**, 1538–1543.

Zwicky, F. (1939). "Cosmic Rays from Supernovae," *Phys. Rev.* **55**, 986.